https://doi.org/10.5194/egusphere-2023-383
Preprint. Discussion started: 24 March 2023

Simulated responses of soil carbon to climate change in CMIP6 Earth System Models: the role of false priming

Rebecca M. Varney[1], Sarah E. Chadburn[1], Eleanor J. Burke[2], Andy J. Wiltshire[2, 3], and Peter M. Cox[1, 3]

[1]Department of Mathematics and Statistics, Faculty of Environment, Science and Economy, University of Exeter, Laver Building, North Park Road, Exeter, EX4 4QE, UK
[2]Met Office Hadley Centre, FitzRoy Road, Exeter, EX1 3PB, UK
[3]Global Systems Institute, University of Exeter, Laver Building, North Park Road, Exeter, EX4 4QE, UK

Correspondence: Rebecca M. Varney (r.varney@exeter.ac.uk)

Abstract. Reliable estimates of soil carbon change are required to determine the carbon budgets consistent with the Paris climate targets. This study evaluates projections of soil carbon during the 21st century in CMIP6 Earth System Models (ESMs) under a range of atmospheric composition scenarios. In general, we find a reduced spread of changes in global soil carbon (ΔC_s) in CMIP6 compared to the previous CMIP5 model generation. However, similar reductions were not seen in the derived contributions to ΔC_s due to both increases in plant Net Primary Productivity (NPP, named $\Delta C_{s,NPP}$) and reductions in the effective soil carbon turnover time (τ_s, named $\Delta C_{s,\tau}$). Instead, we find a strong relationship across the CMIP6 models between these NPP and τ_s components of ΔC_s, with more positive values of $\Delta C_{s,NPP}$ being correlated with more negative values of $\Delta C_{s,\tau}$. We show that this emergent relationship is the result of 'false priming', which leads to a decrease in the effective soil carbon turnover time as a direct result of NPP increase and occurs when the rate of increase of NPP is relatively fast compared to the slower timescales of a multipool soil carbon model. The inclusion of more soil carbon models with multiple pools in CMIP6 compared to CMIP5, therefore seems to have contributed towards the reduction in the overall model spread in future soil carbon projections.

1 Introduction

The response of soil carbon to human-induced climate change represents one of the greatest uncertainties in determining future atmospheric CO_2 concentrations (Canadell et al., 2021). Global soil carbon stocks contain at least 3 times more carbon than present atmospheric concentrations and is the largest store of carbon on the land surface of Earth (Jackson et al., 2017). The land surface has been a carbon sink throughout the 20th century and is estimated to be currently absorbing about 30% of current CO_2 emissions (Friedlingstein et al., 2022). However, the long-term response of soil carbon is uncertain due to large stocks which are known to be particularly sensitive to changes in CO_2 and the subsequent global warming (Cox et al., 2000). For example, permafrost thaw under climate change has the potential to release significant amounts of carbon into the atmosphere over a short period of time with increased warming, representing a significant feedback within the climate system (Schuur et al., 2022; Hugelius et al., 2020; Burke et al., 2017). Therefore, quantifying the future response of soil carbon to increased CO_2 is vital in determining the long-term potential land carbon storage.

https://doi.org/10.5194/egusphere-2023-383
Preprint. Discussion started: 24 March 2023

Soil carbon storage in the future will be determined by the net response of changes in land-atmosphere carbon exchange under increased anthropogenic CO_2. The carbon fluxes which control the fate of global soil carbon stocks are known to be sensitive to changes in climate, and therefore result in soil carbon driven feedbacks to climate change (Canadell et al., 2021). The overall effect of climate change on soil carbon is not very well constrained due to competing feedbacks (Arora et al., 2020, 2013). These include both the negative feedback due to the CO_2 fertilisation effect resulting in increased absorption of carbon by the land surface (Schimel et al., 2015), and the positive climate feedback due to increased carbon losses via soil respiration (Crowther et al., 2016). The balance between these effects will determine the future response of soil carbon stocks under a changing climate (Friedlingstein et al., 2006).

This study assumes Net Primary Productivity (NPP) represents the input flux of carbon to the soil, and is defined as the net rate of accumulation of carbon by vegetation arising from photosynthesis minus the loss from plant respiratory fluxes (Todd-Brown et al., 2014, 2013). NPP is projected to increase under increased atmospheric CO_2 due to the CO_2 fertilization effect, which can result in an increased soil carbon storage (Schimel et al., 2015). Heterotrophic respiration (R_h) is assumed to represent the output flux of carbon from the soil, and is defined as the carbon losses due to decomposition from microbes in the soil. R_h is projected to increase under global warming, where increased global temperatures result in an increased rate of microbial decomposition (Varney et al., 2020). Soil carbon turnover time (τ_s) is defined as the ratio of soil carbon stocks to the output flux of carbon (R_h), where warming alone generally reduces τ_s resulting in a release of carbon from the soil into the atmosphere (Crowther et al., 2016).

In this study, CMIP6 Earth System Models (ESMs) are used to predict changes to soil carbon stocks under future climate scenarios with differing magnitudes of climate change (*SSP126*, *SSP245*, *SSP585*; Eyring et al. (2016); O'Neill et al. (2016)). The aim is to evaluate estimates of soil carbon change (ΔC_s) during the 21st century to: (a) quantify the soil carbon driven feedback to climate change, and (b) enable comparisons with the previous generation of CMIP5 ESMs (*RCP2.6*, *RCP4.5*, *RCP8.5*; Taylor et al. (2012); Meinshausen et al. (2011)). Additionally, this study includes analysis of 21st century carbon fluxes to and from the soil, represented by changes in NPP and τ_s, and investigates how these individual terms contribute to the net soil carbon response projected by ESMs.

2 Methods

2.1 Earth system models

2.1.1 Future climate scenarios

This study uses output data from 10 CMIP6 ESMs (Eyring et al., 2016): ACCESS-ESM1-5, BCC-CSM2-MR, CanESM5, CESM2, CNRM-ESM2-1, IPSL-CM6A-LR, MIROC-ES2L, MPI-ESM1-2-LR, NorESM2-LM, and UKESM1-0-LL. For comparison between the CMIP generations, output data from 9 CMIP5 ESMs is also used (Taylor et al., 2012): BNU-ESM, CanESM2, GFDL-ESM2G, GISS-E2-R, HadGEM2-ES, IPSL-CM5A-LR, MIROC-ESM, MPI-ESM-LR, and NorESM1-M. The ESMs included were chosen due to the availability of the data required at the time of analysis (CMIP6: https://esgf-

https://doi.org/10.5194/egusphere-2023-383
Preprint. Discussion started: 24 March 2023

node.llnl.gov/search/cmip6/, last access: 8 April 2022) and CMIP5: (https://esgf-node.llnl.gov/search/cmip5/, last access: 12 April 2022). Specific soil carbon related updates within ESMs from CMIP5 to CMIP6 are included in Varney et al. (2022) within the 'Earth system models' section of the Methods, and more general model updates are presented within the 'Model descriptions' section of the Arora et al. (2020) Appendix.

The analysis in this study considers 3 future climate scenarios defined by CMIP, which are used to consider different levels of global warming and associated climate policies. The CMIP6 'Shared Socioeconomic Pathways' (SSPs) considered in this study are: *SSP126*, *SSP245*, *SSP585*, which run from 2015 to 2100 (O'Neill et al., 2014; O'Neill et al., 2016). These pathways are chosen to allow for comparison with the CMIP5 'Representative Concentration Pathways' (RCPs): *RCP2.6*, *RCP4.5* and *RCP8.5*, which run from 2005 to 2100 (Meinshausen et al., 2011). It is noted that the SSP and RCP concentration scenarios are not identical, but they are similar enough to enable helpful comparisons between CMIP5 and CMIP6 projections. For the reference period from which change is calculated, the CMIP *Historical* simulation was considered, where the simulation runs from 1850 to 2005 in CMIP5 and from 1850 to 2015 in CMIP6. A change (Δ) was defined as the difference between the last decade of the 21st century (time-averaged between 2090 and 2100) and the last decade of the CMIP5 historical simulation (time-averaged between 1995-2005), which allows for consistency between the CMIP generations. If a timeseries is considered, the historical reference period (historical simulation time-averaged between 1995-2005) was taken away from the entire future climate simulation (e.g. *SSP126* minus the historical reference period).

2.1.2 C4MIP experiments

This study also uses model experiments set up by the Coupled Climate-Carbon Cycle Model Intercomparison Project (C4MIP), which are idealised experiments designed to separate the effects of CO_2 increases and climate change on land and ocean carbon stores. In these experiments additional effects such as land-use change, aerosols or non-CO_2 greenhouse gases are not included, and nitrogen deposition is fixed at pre-industrial values (Jones et al., 2016). The experiments included are: (1) a '*full* 1% CO_2 simulation' (CMIP6 simulation *1pctCO2*), which is a simulation that sees a 1% increase in atmospheric CO_2 per year, starting from pre-industrial concentrations (285 ppm) and running for 150 years, (2) a biogeochemically coupled '*BGC* simulation' (CMIP6 simulation *1pctCO2-bgc*), where the 1% CO_2 increase per year only affects the carbon cycle component of the ESM and the radiative code remains at pre-industrial CO_2 values, and (3) a radiatively coupled '*RAD* simulation' (CMIP6 simulation *1pctCO2-rad*), where the 1% CO_2 increase per year affects only the radiative code and the carbon cycle component on the ESM remains at pre-industrial CO_2 values. These simulations are used with 10 CMIP6 ESMs for further analysis: ACCESS-ESM1-5, BCC-CSM2-MR, CanESM5, CESM2, GFDL-ESM4, IPSL-CM6A-LR, MIROC-ES2L, MPI-ESM1-2-LR, NorESM2-LM, and UKESM1-0-LL, and where '2xCO_2' and 4xCO_2 are defined as 70 and 140 years into the simulations, respectively.

2.1.3 Climate variables

Using ESM output variables, soil carbon (C_s) is defined as the sum of carbon stored in soils and surface litter (CMIP variable *cSoil* + CMIP variable *cLitter*). This allows for a more consistent comparison between the models due to differences in how soil carbon and litter carbon are defined. For models that do not report a separate litter carbon pool (*cLitter*), soil carbon is

https://doi.org/10.5194/egusphere-2023-383
Preprint. Discussion started: 24 March 2023

taken to be simply the *cSoil* variable. Spatial C_s is given in units of kg m^{-2}, and global total C_s is given in units of PgC, which are calculated using an area weighted sum (using the model land surface fraction, CMIP variable *sftlf*).

Additionally, ESM output variables were used to define the soil carbon driven climate feedbacks. Net Primary Productivity (NPP, CMIP variable *npp*) is defined as the net carbon assimilated by plants via photosynthesis minus loss due to plant respiration and is used to represent the net carbon input flux to the system. Heterotrophic Respiration (R_h, CMIP variable *rh*) is defined as the microbial respiration within global soils and is used to define an effective global soil carbon turnover time (τ_s), see Equation 1. τ_s (years) is defined as the ratio of mean soil carbon to annual mean heterotrophic respiration (where the mean represents an area weighted global average). Carbon fluxes (NPP and R_h) are considered as area weighted global totals in units of PgC yr^{-1}.

$$\tau_s = \frac{C_s}{R_h} \tag{1}$$

2.2 Breaking down the projected changes in soil carbon

From Equation 1, soil carbon (C_s) can be defined as shown by Equation 2. Future soil carbon stocks can be defined as initial soil carbon ($C_{s,0}$) plus a change in soil carbon (ΔC_s), as shown by Equation 3, where the subscript 0 denotes the initial state (historical simulation time-averaged between 1995-2005). Equation 3 can be expanded to give Equation 4, which can be simplified to give Equation 5.

$$C_s = R_h \tau_s \tag{2}$$

$$C_{s,0} + \Delta C_s = (R_{h,0} + \Delta R_h)(\tau_{s,0} + \Delta \tau_s) \tag{3}$$

$$C_{s,0} + \Delta C_s = R_{h,0}\tau_{s,0} + \tau_{s,0}\Delta R_h + R_{h,0}\Delta \tau_s + \Delta R_h \Delta \tau_s \tag{4}$$

$$\Delta C_s = \tau_{s,0}\Delta R_h + R_{h,0}\Delta \tau_s + \Delta R_h \Delta \tau_s \tag{5}$$

To isolate the above and below ground effects on soil carbon, the separate effects due to changes in NPP and changes due to τ_s are considered (Todd-Brown et al., 2014). For carbon to be conserved however, the difference between the global fluxes NPP and R_h in a transient climate must be taken into account, where the difference is defined as the Net Ecosystem Productivity (NEP), as shown in Equation 6.

$$\mathrm{NEP} = \mathrm{NPP} - \mathrm{R_h} \tag{6}$$

https://doi.org/10.5194/egusphere-2023-383
Preprint. Discussion started: 24 March 2023

Equation 6 can be substituted into Equation 5, to obtain an equation for ΔC_s in terms of NPP, NEP and τ_s (Equation 7).

$$\Delta C_s = \tau_{s,0}\Delta(\mathrm{NPP} - \mathrm{NEP}) + (\mathrm{NPP}_0 - \mathrm{NEP}_0)\Delta\tau_\mathrm{s} + \Delta(\mathrm{NPP} - \mathrm{NEP})\Delta\tau_\mathrm{s} \tag{7}$$

If the initial state is a steady-state, the initial NEP (NEP_0) will be approximately equal to zero. However, as our initial state is defined as the end of the historical simulation, NEP_0 will therefore be non-zero as a result of the contemporary global land carbon sink. ESMs may also include additional carbon fluxes that cause changes to the resultant soil carbon inputs, such as: grazing, harvest, land-use change, and fire (Todd-Brown et al., 2014). The ΔNEP terms in Equation 7 implicitly includes these effects.

Finally, Equation 7 can expanded to give Equation 8, and the individual responses which make up the total change in soil carbon (ΔC_s) can be broken-down into 6 components:

$$\Delta C_s = \tau_{s,0}\Delta\mathrm{NPP} - \tau_{\mathrm{s},0}\Delta\mathrm{NEP} + \mathrm{NPP}_0\Delta\tau_\mathrm{s} - \mathrm{NEP}_0\Delta\tau_\mathrm{s} + \Delta\mathrm{NPP}\Delta\tau_\mathrm{s} - \Delta\mathrm{NEP}\Delta\tau_\mathrm{s} \tag{8}$$

Equation 7 is exact for given time-varying values of NPP, NEP and τ_s, but in this form it does not cleanly separate into contributions due to changes in each of these factors. A linear approximation is therefore made (assuming $\Delta\mathrm{NPP}/\mathrm{NPP} << 1$ and $\Delta\tau_s/\tau_s << 1$), which allows for the cross-terms to be neglected ($\Delta\mathrm{NPP}\Delta\tau_\mathrm{s}$ and $\Delta\mathrm{NEP}\Delta\tau_\mathrm{s}$). The resultant terms in Equation 8 are defined as given below.

$$\Delta C_{s,NPP} \approx \tau_{s,0}\Delta\mathrm{NPP} \tag{9}$$

$$\Delta C_{s,NEP} \approx -\tau_{s,0}\Delta\mathrm{NEP} \tag{10}$$

$$\Delta C_{s,\tau} \approx \mathrm{NPP}_0\Delta\tau_\mathrm{s} \tag{11}$$

$$\Delta C_{s,\tau_{NEP}} \approx -\mathrm{NEP}_0\Delta\tau_\mathrm{s} \tag{12}$$

Where, $\Delta C_{s,NPP}$ is the change in soil carbon due to changes in NPP, $\Delta C_{s,NEP}$ is the change in soil carbon due to changes in NEP, and $\Delta C_{s,\tau}$ is the change in soil carbon due to changes in τ_s (with $\Delta C_{s,\tau_{NEP}}$ accounting for non-equilibrium).

https://doi.org/10.5194/egusphere-2023-383
Preprint. Discussion started: 24 March 2023

3 Results and Discussion

3.1 Projected changes in soil carbon

A reduced spread in projected end of 21st century estimates of ΔC_s is seen in CMIP6 compared to CMIP5 (Fig. 1). This reduced spread is shown in Fig. 1, where projections of ΔC_s by 2100 in CMIP6 are compared with those from CMIP5 across the different future scenarios. The reduced range of projected changes is seen across all future scenarios (*SSP126* and *RCP2.6*, *SSP245* and *RCP4.5*, *SSP585* and *RCP8.5*), with the range in CMIP6 consistently less than 50% of the equivalent range in CMIP5 (Fig. 1). This reduced spread in projections is also suggested by a reduced standard deviation about the ensemble mean ΔC_s in CMIP6 compared with CMIP5, which is consistently reduced by 50% across all future climate scenarios (Tables 1 and A1, bottom rows). It is noted that the large range in CMIP5 estimates is mostly a result of large increases in C_s in HadGEM2-ES and MPI-ESM-LR, together with the large C_s losses in GISS-E2-R (Fig. 1). An updated CMIP6 version of the GISS-E2-R model is not included in this analysis of this study, which could contribute to the reduced uncertainty from CMIP5. However, the updated equivalent CMIP6 models UKESM1-0-LL (from HadGEM2-ES) and MPI-ESM1-2-LR (from MPI-ESM-LR) have projected estimates of ΔC_s which are more consistent with the other models in the CMIP6 ensemble.

Nearly all of the ESM projections in CMIP6 suggest an increase in C_s by 2100, however CMIP5 models project both increases (positive ΔC_s) and decreases (negative ΔC_s) in soil carbon during the 21st century (Fig. 1). In CMIP5 projections, the future responses of soil carbon range from an increase of 23.2% (HadGEM2-ES) to a decrease of 6.50% (GISS-E2-R) in *RCP8.5*, where across all future scenarios approximately half of the models show increases and half show decreases in ΔC_s (Table A1). In CMIP6, the future responses of soil carbon range from an increase of 12.5% (MPI-ESM1-2-LR) to a decrease of 2.25% (ACCESS-ESM1.5) in *SSP585*, however the majority of models predict an increase in ΔC_s across all future scenarios (Table 1).

Despite more consistent projections of increased ΔC_s in CMIP6 compared with CMIP5, it is apparent that greater CO_2 forcing (i.e. *SSP585* compared with *SSP126*) does not always imply a greater magnitude of increased C_s. By contrast to what is seen in CMIP6, the majority of CMIP5 models project an increased magnitude in estimated ΔC_s with increased CO_2 forcing (Fig. 1). In CMIP6, half the models (CESM2, CNRM-ESM2-1, IPSL-CM6A-LR, NorESM2-LM, and UKESM1-0-LL) estimate less soil carbon accumulation by 2100 (i.e. a smaller increase or a greater decrease) in *SSP585* when compared with *SSP126*. This effect is most prominent in BCC-CSM2-MR and UKESM1-0-LL, where a turning point from increasing to decreasing soil carbon is seen in the mid-century of the *SSP585* projections (Fig. 2). This is opposed to an estimated increase in soil carbon storage with increased forcing, which is generally seen in CMIP5 and the remaining CMIP6 models (CanESM5, MIROC-ES2L, and MPI-ESM1-2-LR). This finding suggests a potential limit to ΔC_s increase and a reduced likelihood of a carbon sink under more extreme levels of climate change.

The spatial pattern of estimated ΔC_s (Fig. 3) is quite variable between CMIP6 ESMs. For example in the tropical regions, where increases in soil carbon can be seen in 6 of the CMIP6 ESMs (BCC-CSM2-MR, CanESM5, CESM2, MIROC-ES2L, and NorESM2-LM), but decreases are seen in the remaining 4 (ACCESS-ESM1-5, CNRM-ESM2-1, IPSL-CM6A-LR, and UKESM1-0-LL). There is a lack of agreement in the high northern latitudes amongst the CMIP6 ESMs (Fig. 3), where it is

https://doi.org/10.5194/egusphere-2023-383
Preprint. Discussion started: 24 March 2023

known that the uncertainty surrounding the fate of soil carbon stocks in these regions is particularly important due to the large magnitude of carbon stored (Burke et al., 2020; Jackson et al., 2017). It has previously been found that a high accumulation of northern latitude C_s is predicted amongst CMIP5 ESMs, however this C_s response has not been suggested in empirical studies (Todd-Brown et al., 2014). The results here suggest that this accumulation (increased ΔC_s) remains in the majority of CMIP6 ESMs (Fig. 3), although reductions in northern latitude soil carbon stocks were found in 3 CMIP6 ESMs (BCC-CSM2-MR, CESM2 and NorESM2-LM, with BCC-CSM2-MR seeing reductions in a greater area). These ESMs which predicted northern latitude C_s reductions were previously found to simulate historical northern latitude soil carbon stocks which are more consistent with the observational estimates seen in these regions (Varney et al., 2022).

3.2 Future changes to land-atmosphere fluxes

The projected ΔC_s is a result of the changing input and output land-atmosphere fluxes under climate change. To a first order, the response of soil carbon will be determined by changes to NPP and to τ_s (see Equation 7). In this section, future projections of these fluxes are analysed in both CMIP6 and CMIP5 ESMs.

3.2.1 Net Primary Productivity

NPP is projected by CMIP6 ESMs to increase during the 21st century, with a greater increase with increasing climate forcing (across SSP scenarios). This result is consistent with the projections of ΔNPP amongst the CMIP5 models (Fig. 4; Todd-Brown et al. (2014)). Projections amongst ESMs however, show disagreement in the magnitude of ΔNPP by 2100 across all future climate scenarios, where a projected CMIP6 ensemble increase of 24.6 $\pm$ 16.9 PgC yr^{-1} is seen in *SSP585*. The largest projections of ΔNPP amongst the CMIP6 models are seen in CanESM5 and BCC-CSM2-MR, where increases of 65.8 PgC yr^{-1} (47% increase) and 39.4 PgC yr^{-1} (43% increase) are projected by 2100 under *SSP585*, respectively. This is compared to ACCESS-ESM1-5 which has the lowest projected changes amongst the CMIP6 models with an increase of only 4.07 PgC yr^{-1} (10% increase) by 2100 under *SSP585* (Table 2).

The CMIP6 ensemble sees a slightly increased range in end of century ΔNPP compared with CMIP5, across all future scenarios (Tables 2 and A2). Fig. 4 suggests that the increased range is mostly due to outlying projections of ΔNPP (CanESM5), where greater increases are seen compared to the majority of models within the ensemble. It is noted that a cluster of ESMs which have similar projections of ΔNPP is seen within CMIP6 (CESM2, MIROC-ES2L, MPI-ESM1-2-LR, NorESM2-LM, and UKESM1-0-LL). The cluster is found to be made up of ESMs which include the simulation of an interactive nitrogen cycle (shown by the dashed lines throughout this study), which is a common addition within CMIP6 ESMs (ACCESS-ESM1.5, CESM2, MIROC-ES2L, MPI-ESM1-2-LR, NorESM2-LM and UKESM1-0-LL; Davies-Barnard et al. (2020)). ACCESS-ESM1-5 is the only model which simulates interactive nitrogen and does not predict consistent ΔNPP with the other nitrogen ESMs in CMIP6, however the projections of ΔNPP in ACCESS-ESM1-5 is consistent with the projections of NorESM1-M in CMIP5, which is the only CMIP5 model considered here to simulate interactive nitrogen (Fig. 4).

https://doi.org/10.5194/egusphere-2023-383
Preprint. Discussion started: 24 March 2023

3.2.2 Soil carbon turnover time

Future τ_s is projected by CMIP6 ESMs to decrease by 2100 across all future SSP scenarios (Fig. 5). A greater reduction in τ_s is seen with increased climate forcing scenario, where a reduced τ_s is a faster soil carbon turnover time, and implies that carbon is cycled back to the atmosphere in less time due to an increased carbon output from the soil (increased R_h, see Equation 1). This result is consistent with the projections of $\Delta\tau_s$ amongst the CMIP5 models (Fig. 5; Todd-Brown et al. (2014)). However, it is found that greater variation exists amongst the CMIP6 ESMs end of century estimates, where a projected CMIP6 ensemble $\Delta\tau_s$ value of -7.65 $\pm$ 5.65 years is seen in *SSP585* compared to -6.13 $\pm$ 3.03 years for CMIP5 ESMs in *RCP8.5* (Tables 2 and A2).

The CMIP6 ESMs with the greatest reductions in effective global τ_s by 2100 is seen in BCC-CSM2-MR, CESM2 and NorESM2-LM, where global carbon turnover in the soil is at least 14 years faster at the end of the *SSP585* simulation compared to the start of the 21st century (historical reference). The CMIP6 models with the least change in effective global τ_s are ACCESS-ESM1-5, IPSL-CM6A-LR, and MPI-ESM1-2-LR, where global carbon turnover in the soil is only around 2 years faster at the end of the *SSP585* simulation (Table 2). The increased range in CMIP6 from CMIP5 is primarily due to the large τ_s reductions seen in the CMIP6 models NorESM2-LM, CESM2 and BCC-CSM2-MR (Fig. 5).

3.3 Breaking down the projected changes in soil carbon

To understand the projected end of century changes in soil carbon storage (ΔC_s) in ESMs, the individual responses of soil carbon due to changes in NPP ($\Delta C_{s,NPP}$, see Equation 9) and the response due to changes in τ_s ($\Delta C_{s,\tau}$, see Equation 12) were diagnosed for both CMIP5 and CMIP6 as shown in Fig. 6. Future ΔC_s (blue bars) is found to mostly a result of the net effect of the linear terms: $\Delta C_{s,NPP}$ (dark green bars) and $\Delta C_{s,\tau}$ (red bars). However, there are also non-negligible contributions from the non-linear term: $\Delta\mathrm{NPP}\Delta\tau_\mathrm{s}$ (black bars), and a small addition due to the non-equilibrium terms: $\Delta C_{s,NEP}$ (light green bars), $\Delta C_{s,\tau_{NEP}}$ (pink bars), and $\Delta\mathrm{NEP}\Delta\tau_\mathrm{s}$ (grey bars).

The importance of investigating the individual processes which contribute to the net ΔC_s in ESMs can be seen (Fig. 6). In Fig. 6 it is seen that the net ΔC_s is relatively small compared to the individual changes from the derived components, where especially large magnitudes are seen in the increased C_s due to increased ΔNPP ($\Delta C_{s,NPP}$) and the decreased C_s due to reduced $\Delta\tau_s$ ($\Delta C_{s,\tau}$). For example, in *SSP585* there is a range of approximately 170 PgC in net ΔC_s, from an increase of 132 PgC (CNRM-ESM2-1) to a reduction of 35 PgC (BCC-CSM2-MR). However, the $\Delta C_{s,NPP}$ contribution has a much larger range of 1442 PgC, from an increase of 95 PgC (ACCESS-ESM1-5) to an increase of 1517 PgC (NorESM2-LM). Similarly, $\Delta C_{s,\tau}$ has a range of 756 PgC, from a decrease of 115 PgC (ACCESS-ESM1-5) to a decrease of 871 PgC (NorESM2-LM).

The magnitude of change seen from the individual feedbacks ($\Delta C_{s,NPP}$ and $\Delta C_{s,\tau}$) is not obviously related to the resultant magnitude of soil carbon change (Fig. A1). For example, NorESM2-LM projects large $\Delta C_{s,NPP}$ and $\Delta C_{s,\tau}$ values (1517 PgC and -871 PgC in *SSP585*, respectively), however a relatively small net change in soil carbon (49 PgC in *SSP585*). Conversely, CNRM-ESM2-1 projects smaller $\Delta C_{s,NPP}$ and $\Delta C_{s,\tau}$ values (667 PgC and -413 PgC in *SSP585*, respectively), but a larger net soil carbon change (132 PgC in *SSP585*). Within ESMs, it is found that the change in soil carbon is determined by the

https://doi.org/10.5194/egusphere-2023-383
Preprint. Discussion started: 24 March 2023

relationship between all the contributing terms to the net ΔC_s response, as opposed to the absolute size of a given contribution (Fig. 6).

Surprisingly, a very strong correlation is found amongst the ESMs in CMIP6 (r^2 value of 0.97) between the linear terms $\Delta C_{s,NPP}$ and $\Delta C_{s,\tau}$ (Fig. 7(a)). This leads to the partially cancelling of the terms, with a resultant relatively small net ΔC_s. When comparing with the CMIP5 ensemble, a lower correlation between $\Delta C_{s,NPP}$ and $\Delta C_{s,\tau}$ is seen (r^2 value of 0.084, Fig. 7(a)). This correlation amongst CMIP6 ESMs results in net ΔC_s being more clustered in CMIP6 compared to CMIP5 (Fig. 1), despite a similarly large variation in the individual contributions (Fig. 6). The strong CMIP6 correlation ($r^2 = 0.97$) remains when the fractional changes ($\Delta C_{s,NPP}/C_{s,0}$ and $\Delta C_{s,\tau_{NPP}}/C_{s,0}$, where $C_{s,0}$ is initial soil carbon stocks) are plotted instead (Fig. 7(b)).

Fig. 6 also shows that the differences in ESM projections of ΔC_s are partly due to differing magnitudes of the non-linear term ($\Delta\mathrm{NPP}\Delta\tau_\mathrm{s}$). The non-linear $\Delta\mathrm{NPP}\Delta\tau_\mathrm{s}$ term having non-negligible contributions to future ΔC_s means the initial $\Delta\mathrm{NPP}/\mathrm{NPP} << 1$ and $\Delta\tau_s/\tau_s << 1$ assumptions were not valid in this case. The ESM projected magnitudes of $\Delta\mathrm{NPP}\Delta\tau_\mathrm{s}$ are found to be relatively large, especially in the more extreme climate scenarios (Fig. 6). In *SSP585*, a range from a decreased C_s of 11 PgC (ACCESS-ESM1-5) to a decreased C_s of 599 PgC (BCC-CSM2-MR) is found amongst the CMIP6 models due to only the $\Delta\mathrm{NPP}\Delta\tau_\mathrm{s}$ term, and in some cases values greater magnitudes are seen than the net ΔC_s (BCC-CSM2-MR, CanESM5, CESM2, NorESM2-LM, and UKESM1-0-LL). The term is greater when there are large and counteracting magnitudes of $\Delta\mathrm{NPP}$ and $\Delta\tau_s$, which results in a non-negligible product.

Additionally, to obtain the overall change in soil carbon seen in the models, contributions from the non-equilibrium terms ($\Delta C_{s,NEP}$, $\Delta C_{s,\tau_{NEP}}$, and $\Delta\mathrm{NEP}\Delta\tau_\mathrm{s}$) must also be included (Fig. 6). The $\Delta C_{s,NEP}$ term represents the change in soil carbon due to the net carbon sink during the 21$^{\mathrm{st}}$ century, which exists while the climate is in a transient state due to continuous climate change. By definition, the magnitude of $\Delta C_{s,NEP}$ is negative if $\Delta\mathrm{NEP}$ is positive, which implies a greatest or faster increase in NPP with respect to R_h seen in the majority of ESMs. The contribution from these terms is found to be relatively small in most models, but not in all. In *SSP585*, projections of $\Delta C_{s,NEP}$ amongst CMIP6 models range from a reduction of 333 PgC (NorESM2-LM) to a gain of 8.74 PgC (ACCESS-ESM1-5). In CMIP5, exceptions where greater $\Delta C_{s,NEP}$ terms are found in the GISS-E2-R and MPI-ESM-LR models, implying the models are far from equilibrium at the end of the century. The change in soil carbon due to the change in NEP ($\Delta C_{s,NEP}$) is often found to be greater in the models which see greater magnitudes of $\Delta C_{s,NPP}$ and $\Delta C_{s,\tau}$.

3.4 Investigating the emergent relationship between $\Delta C_{s,NPP}$ and $\Delta C_{s,\tau}$

In this subsection, the emergent relationship between $\Delta C_{s,NPP}$ and $\Delta C_{s,\tau}$ present across the CMIP6 ensemble is further investigated using the idealised C4MIP simulations (see Methods). Fig. 8 presents the relationship between $\Delta C_{s,NPP}$ and $\Delta C_{s,\tau}$ for each CMIP6 ESMs as in Fig. 7, but for the *full* 1% CO_2, *BGC*, and *RAD* simulations. It is found that $\Delta C_{s,NPP}$ and $\Delta C_{s,\tau}$ are strongly correlated in the *full* 1% CO_2 simulation, at both 2xCO_2 (r^2 value of 0.925) and 4xCO_2 (r^2 value of 0.839). The correlation is found to remain in the *BGC* simulation, where r^2 values are found to be 0.838 and 0.708 for 2xCO_2 and 4xCO_2, respectively. The slightly reduced correlation in the *BGC* simulation at 4xCO_2 suggests a potential limit to the effect

https://doi.org/10.5194/egusphere-2023-383
Preprint. Discussion started: 24 March 2023

at high levels of atmospheric CO_2. A correlation is also seen in the *RAD* simulation at 2xCO_2 (r^2 value of 0.601), however the correlation in the *RAD* simulation does not hold at 4xCO_2, where the r^2 value reduces to 0.265. The reduced correlation in the *RAD* simulation at 4xCO_2 suggests a reduced relationship between NPP and τ_s at the more extreme temperature changes that are projected at high levels of atmospheric CO_2.

For each CMIP6 ESM, NPP and τ_s are found to be strongly inversely correlated in the *full* 1% CO_2 simulation (Fig. 9). The r^2 values between $\mathrm{NPP}/\mathrm{NPP}_0$ and $\tau_{s,0}/\tau_s$ (where the subscript 0 denotes the historical state) are found to be greater than 0.95 in all models except for ACCESS-ESM1-5 (where an r^2 value of 0.65 is found due to a breakdown at high CO_2 levels). In the *BGC* simulation, a similar relationship between $\mathrm{NPP}/\mathrm{NPP}_0$ and $\tau_{s,0}/\tau_s$ is seen up until approximately 2xCO_2 in all ESMs (approximately 50% of the simulation). However, how the relationship between $\mathrm{NPP}/\mathrm{NPP}_0$ and $\tau_{s,0}/\tau_s$ changes throughout the *BGC* simulation (between 2xCO_2 and 4xCO_2) varies between models. A greater rate of $\mathrm{NPP}/\mathrm{NPP}_0$ increase compared to $\tau_{s,0}/\tau_s$ is seen at greater levels of climate forcing for the majority of CMIP6 ESMs (BCC-CSM2-MR, CanESM5, GFDL-ESM4, IPSL-CM6A-LR, MIROC-ES2L, MPI-ESM1-2-LR and UKESM1-0-LL), where the τ_s changes appear to saturate and a limit to the increase is seen. In these ESMs, the changes seen in the *full* and *BGC* simulations differ due to a climate effect (shown by the *RAD* simulation), which appears to negate the apparent limit or saturation seen in the $\tau_{s,0}/\tau_s$ increase in the *BGC* simulation (Fig. 9). In CESM2 and NorESM2-LM (containing the same land surface model component), a consistent relationship is seen in both the *full* 1% CO_2 and *BGC* simulations, suggesting the changes in NPP and τ_s are primarily due to changes in CO_2 concentrations, or that the climate affects cancel out to a resultant net zero change. In ACCESS-ESM1-5, a consistent relationship is seen in the *full* 1% CO_2, *BGC* and *RAD* simulations, suggesting a greater sensitivity of NPP to environmental climate changes compared to the other CMIP6 ESMs (Fig. 9).

Koven et al. (2015) presents the concept of 'false priming', which describes a reduction in effective carbon turnover (τ_s) due to increases in productivity (NPP). It was defined as false priming due to the impact being similar to the 'true priming' process, but occurs without simulating the priming mechanisms; where priming is defined as the stimulation of decomposition of soil carbon (reducing τ_s) due to input of carbon to the soil (Liu et al., 2020). The false priming reduction in effective τ_s is a transient phenomenon that arises in soil models that represent multiple carbon pools with different turnover times. Under continually increasing NPP, proportionally more of the additional input litter carbon is put into the faster soil carbon pools than the slow, which brings down the global average effective τ_s value of the soil.

In this subsection, false priming is explored as a possible explanation for the correlations seen between NPP changes and τ_s changes, which are seen even in the *BGC* simulations where the climate does not change significantly (second row of Fig. 8). Koven et al. (2015) demonstrates false priming with a simple three-box soil carbon model, which has been adapted here to use notation consistent with the rest of this study:

https://doi.org/10.5194/egusphere-2023-383
Preprint. Discussion started: 24 March 2023

$$\frac{dC_{s,1}}{dt} = NPP - \frac{C_{s,1}}{\tau_{s,1}} \tag{13}$$

$$\frac{dC_{s,2}}{dt} = \frac{e_1 C_{s,1}}{\tau_{s,1}} - \frac{C_{s,2}}{\tau_{s,2}} \tag{14}$$

$$\frac{dC_{s,3}}{dt} = \frac{e_2 C_{s,2}}{\tau_{s,2}} - \frac{C_{s,3}}{\tau_{s,3}} \tag{15}$$

$$R_h = \frac{(1-e_1)C_{s,1}}{\tau_{s,1}} + \frac{(1-e_2)C_{s,2}}{\tau_{s,2}} + \frac{(1-e_3)C_{s,3}}{\tau_{s,3}} \tag{16}$$

$$C_s = C_{s,1} + C_{s,2} + C_{s,3} \tag{17}$$

$$\tau_{s,1} = 1, \tau_{s,2} = 10, \tau_{s,3} = 100, e_1 = 0.3, e_2 = 0.3, e_3 = 0. \tag{18}$$

where, $C_{s,1}$, $C_{s,2}$, $C_{s,3}$ represent the carbon stored in soil carbon pools 1, 2, and 3 and make up the total soil carbon (C_s). Similarly, $\tau_{s,i}$ are the respective soil carbon turnover times, which are given defined values of increasing turnover times in years: fast (1 year), medium (10 years) and slow (100 years). NPP represents the carbon input into the system, where carbon is inputted into pool 1 ($C_{s,1}$), then flows to pool 2 ($C_{s,2}$) and then 3 ($C_{s,3}$). The coefficients e_i represents the fraction of carbon that is passed to the next pool rather than outputted as heterotrophic respiration (R_h).

At equilibrium, the change in the soil carbon pools will be zero ($dC_{s,i}/dt = 0$), so the amount of soil carbon present within each pool depends on the input carbon and turnover time of the pool ($\tau_{s,i}$). Under increasing NPP, the three-box model can be used to investigate the subsequent changes to soil carbon in the 3 carbon pools ($C_{s,1}$, $C_{s,2}$, $C_{s,3}$) based on changing input alone, due to each pool having a fixed $\tau_{s,i}$ value. This removes the $\Delta\tau_s$ from changing environmental and microbial conditions (Koven et al., 2015; Wieder et al., 2015; Exbrayat et al., 2013). Fig. 10(a) produces a simulation of the response of this three-box model to an NPP input flux that increases at 0.3% per year (reproducing Fig. 12 in Koven et al. (2015)). The false priming decline in effective τ_s with increasing NPP is clear, and for this set of parameters offsets about 40% of the increase in soil carbon that would arise from the NPP increase alone. Fig. 10(b) demonstrates that false priming is a transient effect associated with a disequilibrium in the distribution of soil carbon between the 3 pools. It shows results from the same model, but for a step increase in global NPP from 50 PgC yr^{-1} to 70 PgC yr^{-1} at year 100. The instantaneous decline in τ_s of about 10% eventually reduces to return the soil to the original τ_s, but this occurs on the timescale of the slowest carbon pool and so may take many centuries.

The same three-box model can also be used to investigate the relationship between the contributions of changes in NPP ($\Delta C_{s,NPP}$) and τ_s ($\Delta C_{s,\tau}$) to net soil carbon change that was noted in both Fig. 7 and Fig. 8. Fig. 11 plots $\Delta C_{s,NPP}$ against $\Delta C_{s,\tau}$ from the three-box model after 70 years of runs that assume different rates of increase of NPP (0% to 0.8% per year in

https://doi.org/10.5194/egusphere-2023-383
Preprint. Discussion started: 24 March 2023

increments of 0.05%). A clear relationship between $\Delta C_{s,NPP}$ and $\Delta C_{s,\tau}$ is seen, with greater false priming (more negative $\Delta C_{s,\tau}$) when the NPP increase is larger (more positive $\Delta C_{s,NPP}$). The similarity of Fig. 11 to both Fig. 7 and Fig. 8 is clear, suggesting that these correlations in CMIP6 (and to a lesser extent in CMIP5) are predominantly due to false priming.

It is noted that the influence of false priming was stronger in the *full* 1% CO_2 and *BGC* (CO_2 only) simulations, compared to the *RAD* (climate only) simulation. This is likely due to the *RAD* simulation not seeing sufficient NPP change for the false priming affect to be significant (see Fig. A2), opposed to false priming being a direct result of atmospheric CO_2 change. Additionally, the direct effect of temperature changes on τ_s in the *RAD* simulation is likely to dampen the correlation to NPP changes, due to both direct and indirect $\Delta\tau_s$ in this case (Varney et al., 2020).

4 Conclusions

In this study, future projections of soil carbon change (ΔC_s) have been analysed using ESM output from the latest CMIP6 ensemble and were investigated under differing levels of climate change (future scenarios *SSP126*, *SSP245* and *SSP585*). The future projections made by CMIP6 ESMs were also compared against equivalent projections made by the previous generation of ESMs in the CMIP5 ensemble (future scenarios *RCP2.6*, *RCP4.5* and *RCP8.5*) to investigate whether recent model improvements have reduced the uncertainty surrounding the future soil carbon response. Additionally, ΔC_s was broken down into the individual components which contribute to the net change within ESMs, with a specific focus on increases due to increases in NPP ($\Delta C_{s,NPP}$) and decreases due to reductions in turnover ($\Delta C_{s,\tau}$). Below the key conclusions from this study are listed:

1. An apparent reduction in uncertainty of end of 21st century ΔC_s projections is suggested in CMIP6 compared to CMIP5.

2. However, the same reduction in projection uncertainty is not suggested surrounding the soil carbon controls: Net Primary Productivity (NPP) and the effective soil carbon turnover time ($\tau_s = C_s/R_h$), and the subsequent effects on future soil carbon storage ($\Delta C_{s,NPP}$ and $\Delta C_{s,\tau}$, respectively).

3. It is noted that the results in this study suggest the inclusion of a interactive nitrogen cycle within simulations constrains the future responses to NPP and shows progress in CMIP6 models.

4. The derived linear terms which contribute to net soil carbon change, the response of soil carbon due to changes in NPP ($\Delta C_{s,NPP}$) and the response due to changes in τ_s ($\Delta C_{s,\tau}$), are found to have a strong relationship in CMIP6, with a more significant correlation than what was seen in CMIP5. This correlation is likely to be a cause of the reduction in the ΔC_s projection spread across the CMIP6 ensemble.

5. The apparent emergent relationship between $\Delta C_{s,NPP}$ and $\Delta C_{s,\tau}$ in CMIP6 ESMs was found to be a result of false priming, which describes a transient increase in effective turnover time due to increased input of carbon to the soil. The net effect of false priming is a coupling affect between ΔNPP and $\Delta\tau_s$, and results in a reduced range of future ΔC_s predictions in CMIP6.

https://doi.org/10.5194/egusphere-2023-383
Preprint. Discussion started: 24 March 2023

6. It is recommended that the full extent of false priming on future soil carbon is understood, where if increased carbon inputs to soil carbon pools preferentially enters fast soil carbon pools, this could limit the maximum increase in soil carbon storage in the future.

Understanding and quantifying soil carbon feedbacks under anthropogenic emissions of CO_2 is critical for calculating an accurate global carbon budget, which is required if Paris Agreement targets are to be met (Friedlingstein et al., 2022). This study highlights the importance of considering the individual soil driven carbon feedbacks under climate change when determining the overall response of global soil carbon storage, and suggests the need for constraints on the magnitudes of these feedbacks in CMIP6 to reduce uncertainty in projections of future land carbon storage.

Code availability. Code is available on GitHub (https://github.com/rebeccamayvarney/CMIP6_dCs).

Data availability. The CMIP data analysed during this study are available online: CMIP6 (https://esgf-node.llnl.gov/search/cmip6/) and CMIP5 (https://esgf-node.llnl.gov/search/cmip5/).

Author contributions. RMV, SEC and PMC outlined the study. RMV completed the analysis and produced the figures. All the co-authors provided guidance on the study at various times and suggested edits to the draft manuscript.

Competing interests. The authors have declared no competing interests.

Acknowledgements. This research has been supported by the European Research Council, Emergent Constraints on Climate–Land feedbacks in the Earth System project (ECCLES; grant no. 742472) and Climate–Carbon Interactions in the Current Century project (4C; grant no. 821003) (RMV and PMC). SEC was supported by a Natural Environment Research Council independent research fellowship (grant no. NE/R015791/1). AJW and EJB were supported by the Joint UK BEIS/Defra Met Office Hadley Centre Climate Programme (grant no. GA01101). We thank the World Climate Research Programme's Working Group on Coupled Modelling and the climate modelling groups for producing and making their model output available.

https://doi.org/10.5194/egusphere-2023-383
Preprint. Discussion started: 24 March 2023

References

Arora, V. K., Boer, G. J., Friedlingstein, P., Eby, M., Jones, C. D., Christian, J. R., Bonan, G., Bopp, L., Brovkin, V., Cadule, P., et al.: Carbon–concentration and carbon–climate feedbacks in CMIP5 Earth system models, Journal of Climate, 26, 5289–5314, 2013.

Arora, V. K., Katavouta, A., Williams, R. G., Jones, C. D., Brovkin, V., Friedlingstein, P., Schwinger, J., Bopp, L., Boucher, O., Cadule, P., et al.: Carbon–concentration and carbon–climate feedbacks in CMIP6 models and their comparison to CMIP5 models, Biogeosciences, 17, 4173–4222, 2020.

Burke, E. J., Ekici, A., Huang, Y., Chadburn, S. E., Huntingford, C., Ciais, P., Friedlingstein, P., Peng, S., and Krinner, G.: Quantifying uncertainties of permafrost carbon–climate feedbacks, Biogeosciences, 14, 3051–3066, 2017.

Burke, E. J., Zhang, Y., and Krinner, G.: Evaluating permafrost physics in the Coupled Model Intercomparison Project 6 (CMIP6) models and their sensitivity to climate change, The Cryosphere, 14, 3155–3174, 2020.

Canadell, J., Monteiro, P., Costa, M., Cotrim da Cunha, L., Cox, P., Eliseev, A., Henson, S., Ishii, M., Jaccard, S., Koven, C., Lohila, A., Patra, P., Piao, S., Rogelj, J., Syampungani, S., Zaehle, S., and Zickfeld, K.: Global Carbon and other Biogeochemical Cycles and Feedbacks, Cambridge University Press, Cambridge, United Kingdom and New York, NY, USA, https://doi.org/10.1017/9781009157896.007, 2021.

Cox, P. M., Betts, R. A., Jones, C. D., Spall, S. A., and Totterdell, I. J.: Acceleration of global warming due to carbon-cycle feedbacks in a coupled climate model, Nature, 408, 184, 2000.

Crowther, T. W., Todd-Brown, K. E., Rowe, C. W., Wieder, W. R., Carey, J. C., Machmuller, M. B., Snoek, B., Fang, S., Zhou, G., Allison, S. D., et al.: Quantifying global soil carbon losses in response to warming, Nature, 540, 104, 2016.

Davies-Barnard, T., Meyerholt, J., Zaehle, S., Friedlingstein, P., Brovkin, V., Fan, Y., Fisher, R. A., Jones, C. D., Lee, H., Peano, D., et al.: Nitrogen cycling in CMIP6 land surface models: progress and limitations, Biogeosciences, 17, 5129–5148, 2020.

Exbrayat, J.-F., Pitman, A., Zhang, Q., Abramowitz, G., and Wang, Y.-P.: Examining soil carbon uncertainty in a global model: response of microbial decomposition to temperature, moisture and nutrient limitation, Biogeosciences, 10, 7095–7108, 2013.

Eyring, V., Bony, S., Meehl, G. A., Senior, C. A., Stevens, B., Stouffer, R. J., and Taylor, K. E.: Overview of the Coupled Model Intercomparison Project Phase 6 (CMIP6) experimental design and organization, Geoscientific Model Development (Online), 9, 2016.

Friedlingstein, P., Cox, P., Betts, R., Bopp, L., von Bloh, W., Brovkin, V., Cadule, P., Doney, S., Eby, M., Fung, I., et al.: Climate–carbon cycle feedback analysis: results from the C4MIP model intercomparison, Journal of climate, 19, 3337–3353, 2006.

Friedlingstein, P., O'sullivan, M., Jones, M. W., Andrew, R. M., Gregor, L., Hauck, J., Le Quéré, C., Luijkx, I. T., Olsen, A., Peters, G. P., et al.: Global carbon budget 2022, Earth System Science Data, 14, 4811–4900, 2022.

Hugelius, G., Loisel, J., Chadburn, S., Jackson, R. B., Jones, M., MacDonald, G., Marushchak, M., Olefeldt, D., Packalen, M., Siewert, M. B., et al.: Large stocks of peatland carbon and nitrogen are vulnerable to permafrost thaw, Proceedings of the National Academy of Sciences, 117, 20 438–20 446, 2020.

Jackson, R. B., Lajtha, K., Crow, S. E., Hugelius, G., Kramer, M. G., and Piñeiro, G.: The ecology of soil carbon: pools, vulnerabilities, and biotic and abiotic controls, Annual Review of Ecology, Evolution, and Systematics, 48, 419–445, 2017.

Jones, C. D., Arora, V., Friedlingstein, P., Bopp, L., Brovkin, V., Dunne, J., Graven, H., Hoffman, F., Ilyina, T., John, J. G., et al.: C4MIP–The coupled climate–carbon cycle model intercomparison project: Experimental protocol for CMIP6, Geoscientific Model Development, 9, 2853–2880, 2016.

https://doi.org/10.5194/egusphere-2023-383
Preprint. Discussion started: 24 March 2023

Koven, C. D., Chambers, J. Q., Georgiou, K., Knox, R., Negron-Juarez, R., Riley, W. J., Arora, V. K., Brovkin, V., Friedlingstein, P., and Jones, C. D.: Controls on terrestrial carbon feedbacks by productivity versus turnover in the CMIP5 Earth System Models, Biogeosciences, 12, 5211–5228, https://doi.org/10.5194/bg-12-5211-2015, 2015.

Liu, X.-J. A., Finley, B. K., Mau, R. L., Schwartz, E., Dijkstra, P., Bowker, M. A., and Hungate, B. A.: The soil priming effect: Consistent across ecosystems, elusive mechanisms, Soil Biology and Biochemistry, 140, 107 617, 2020.

Meinshausen, M., Smith, S. J., Calvin, K., Daniel, J. S., Kainuma, M., Lamarque, J.-F., Matsumoto, K., Montzka, S., Raper, S., Riahi, K., et al.: The RCP greenhouse gas concentrations and their extensions from 1765 to 2300, Climatic change, 109, 213, 2011.

O'Neill, B. C., Tebaldi, C., Vuuren, D. P. v., Eyring, V., Friedlingstein, P., Hurtt, G., Knutti, R., Kriegler, E., Lamarque, J.-F., Lowe, J., et al.: The scenario model intercomparison project (ScenarioMIP) for CMIP6, Geoscientific Model Development, 9, 3461–3482, 2016.

O'Neill, B. C., Kriegler, E., Riahi, K., Ebi, K. L., Hallegatte, S., Carter, T. R., Mathur, R., and van Vuuren, D. P.: A new scenario framework for climate change research: the concept of shared socioeconomic pathways, Climatic change, 122, 387–400, 2014.

Schimel, D., Stephens, B. B., and Fisher, J. B.: Effect of increasing CO2 on the terrestrial carbon cycle, Proceedings of the National Academy of Sciences, 112, 436–441, 2015.

Schuur, E. A., Abbott, B. W., Commane, R., Ernakovich, J., Euskirchen, E., Hugelius, G., Grosse, G., Jones, M., Koven, C., Leshyk, V., et al.: Permafrost and climate change: carbon cycle feedbacks from the warming Arctic, Annual Review of Environment and Resources, 47, 343–371, 2022.

Taylor, K. E., Stouffer, R. J., and Meehl, G. A.: An overview of CMIP5 and the experiment design, Bulletin of the American Meteorological Society, 93, 485–498, 2012.

Todd-Brown, K., Randerson, J., Post, W., Hoffman, F., Tarnocai, C., Schuur, E., and Allison, S.: Causes of variation in soil carbon simulations from CMIP5 Earth system models and comparison with observations, Biogeosciences, 10, 1717–1736, 2013.

Todd-Brown, K., Randerson, J., Hopkins, F., Arora, V., Hajima, T., Jones, C., Shevliakova, E., Tjiputra, J., Volodin, E., Wu, T., et al.: Changes in soil organic carbon storage predicted by Earth system models during the 21st century, Biogeosciences, 11, 2341–2356, 2014.

Varney, R. M., Chadburn, S. E., Friedlingstein, P., Burke, E. J., Koven, C. D., Hugelius, G., and Cox, P. M.: A spatial emergent constraint on the sensitivity of soil carbon turnover to global warming, Nature communications, 11, 1–8, 2020.

Varney, R. M., Chadburn, S. E., Burke, E. J., and Cox, P. M.: Evaluation of soil carbon simulation in CMIP6 Earth system models, Biogeosciences, 19, 4671–4704, https://doi.org/10.5194/bg-19-4671-2022, 2022.

Wieder, W. R., Allison, S. D., Davidson, E. A., Georgiou, K., Hararuk, O., He, Y., Hopkins, F., Luo, Y., Smith, M. J., Sulman, B., et al.: Explicitly representing soil microbial processes in Earth system models, Global Biogeochemical Cycles, 29, 1782–1800, 2015.

https://doi.org/10.5194/egusphere-2023-383
Preprint. Discussion started: 24 March 2023

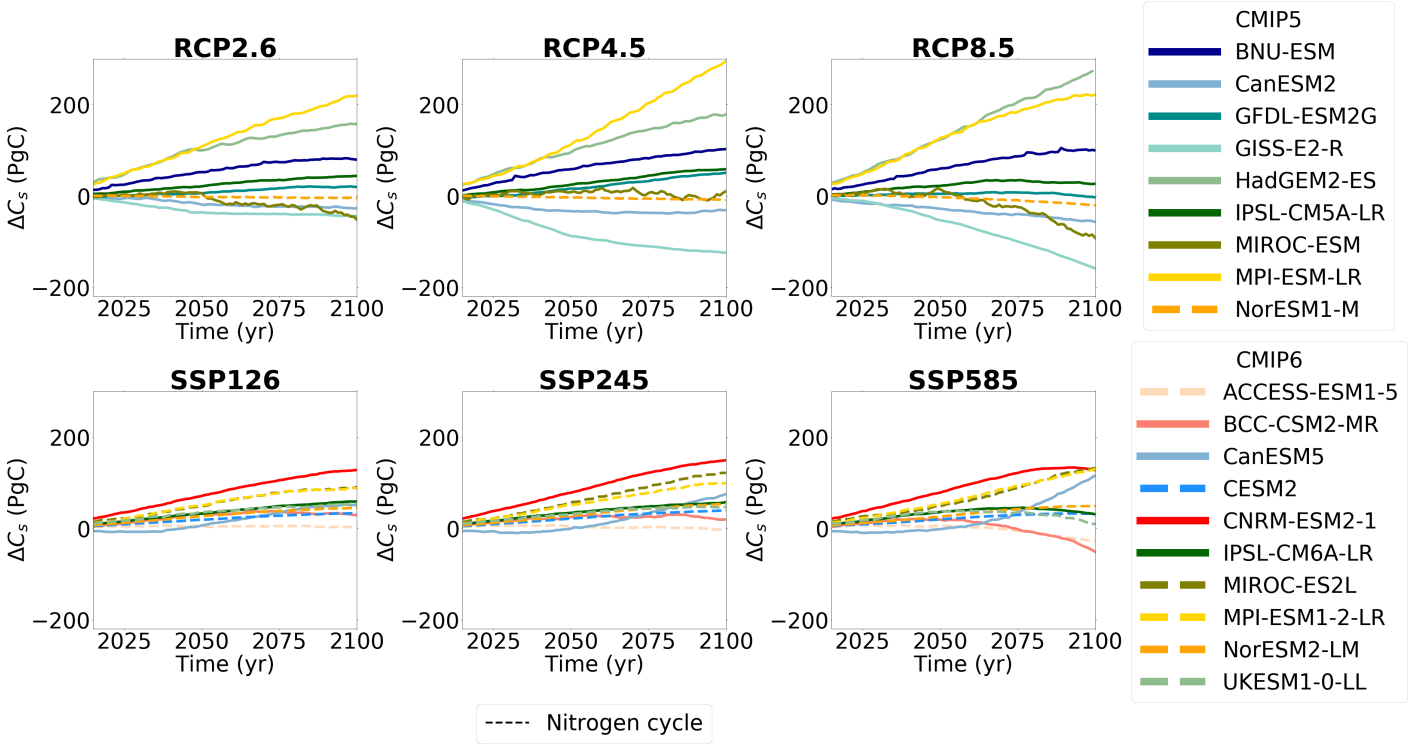

Figure 1. Projected future change in soil carbon (ΔC_s) in CMIP5 (top row) and CMIP6 (bottom row) ESMs, for future climate scenarios *RCP2.6* and *SSP126*, *RCP4.5* and *SSP245*, *RCP8.5* and *SSP585*, respectively. The dashed lines represent ESMs which include the representation of interactive nitrogen in these simulations.

https://doi.org/10.5194/egusphere-2023-383
Preprint. Discussion started: 24 March 2023

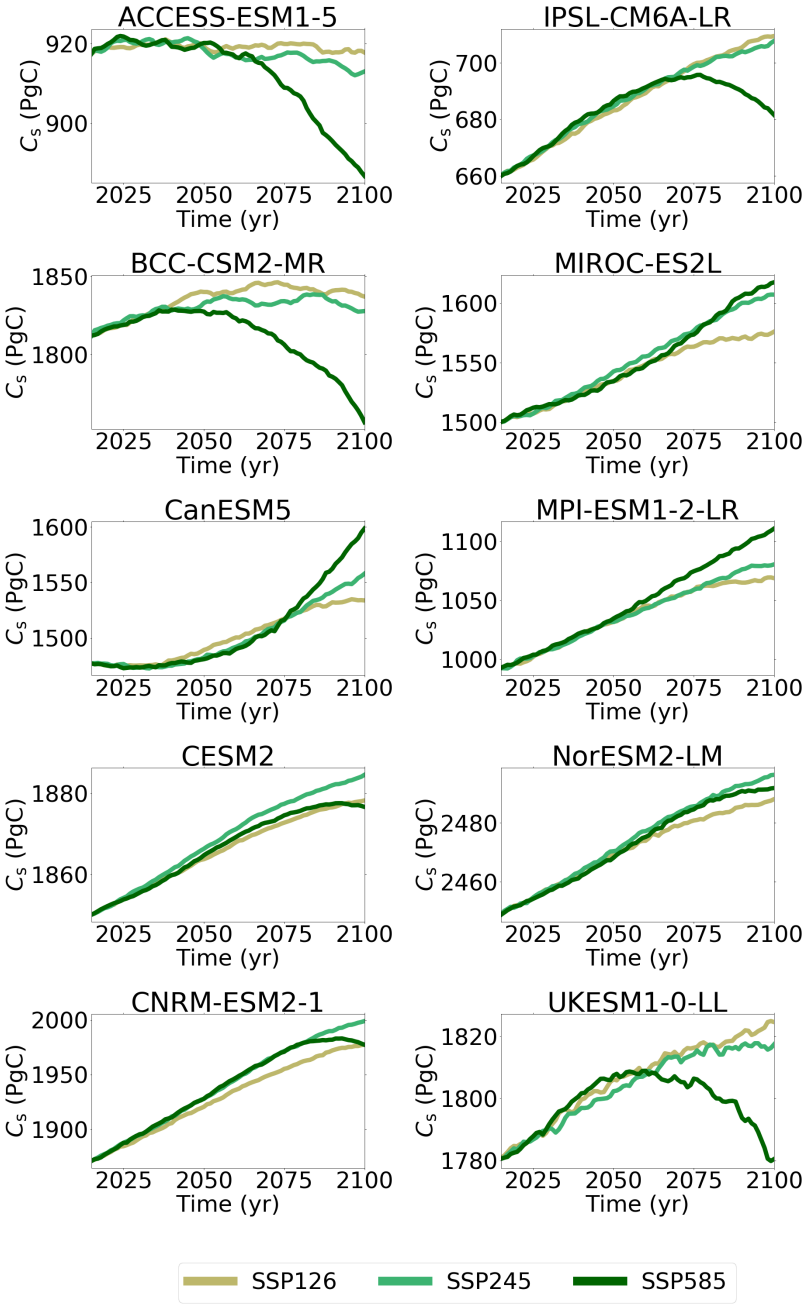

Figure 2. Timeseries of projected future soil carbon (C_s) in CMIP6 ESMs for future climate scenarios *SSP126*, *SSP245*, *SSP585*.

https://doi.org/10.5194/egusphere-2023-383
Preprint. Discussion started: 24 March 2023

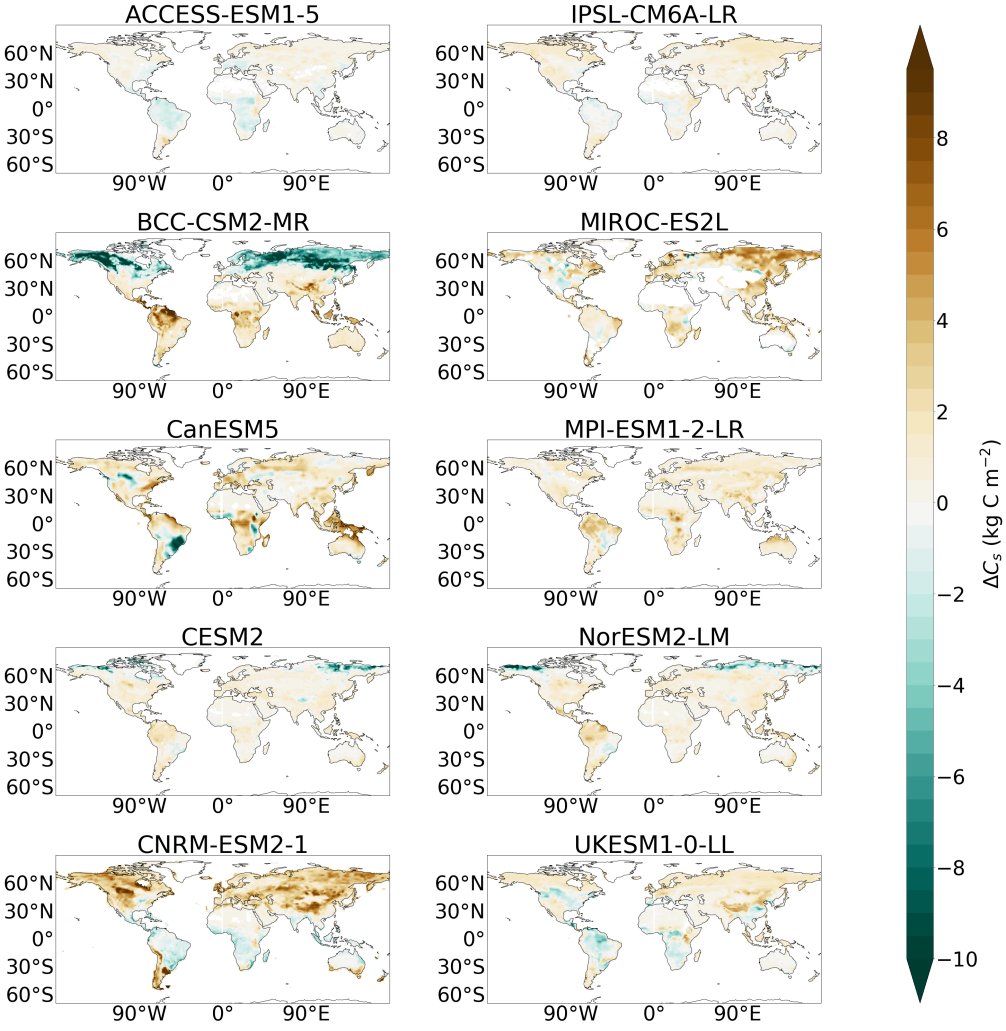

Figure 3. Map plots showing the change in soil carbon (ΔC_s) in *SSP585* for each CMIP6 ESM.

https://doi.org/10.5194/egusphere-2023-383
Preprint. Discussion started: 24 March 2023

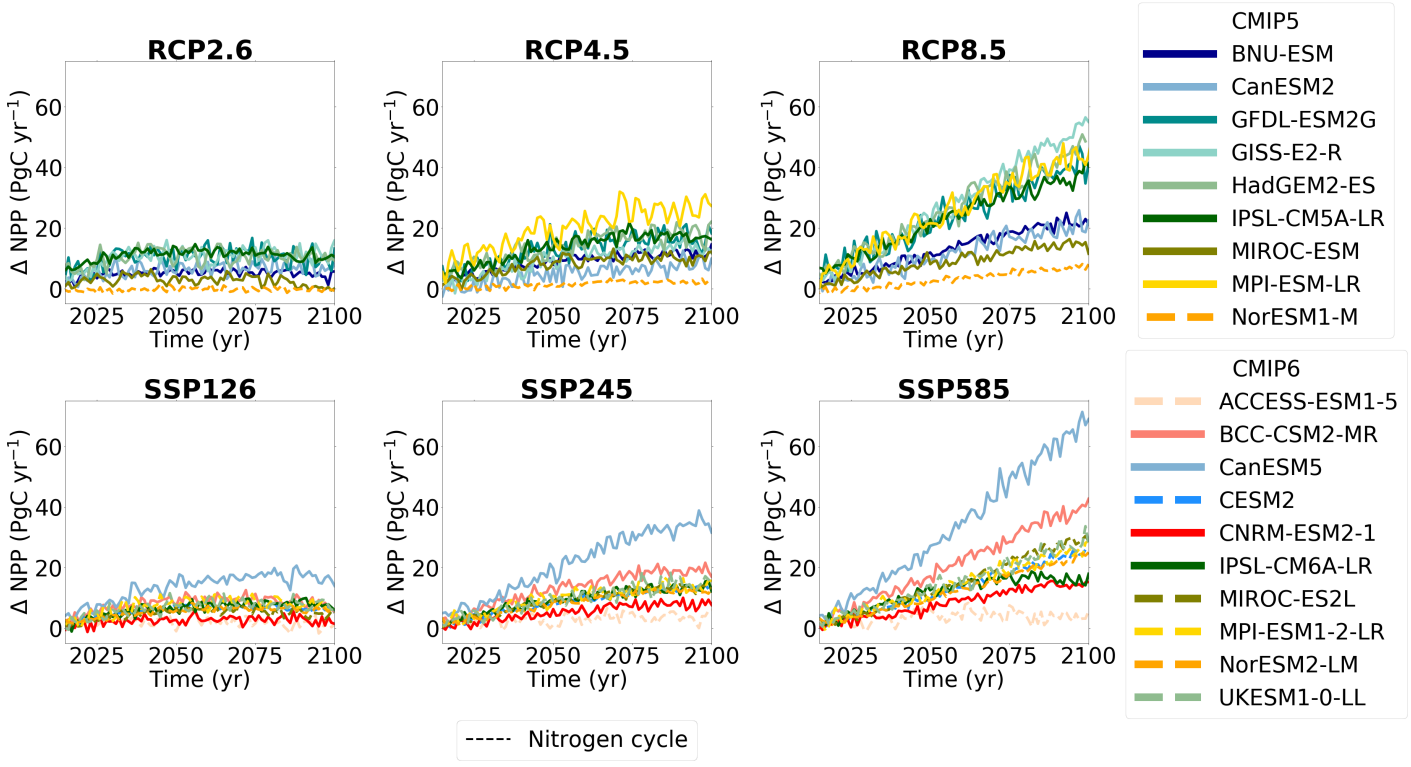

Figure 4. Projected future change in Net Primary Production (ΔNPP) in CMIP5 (top row) and CMIP6 (bottom row) ESMs, for future climate scenarios *RCP2.6* and *SSP126*, *RCP4.5* and *SSP245*, *RCP8.5* and *SSP585*, respectively. The dashed lines represent ESMs which include the representation of interactive nitrogen in these simulations.

https://doi.org/10.5194/egusphere-2023-383
Preprint. Discussion started: 24 March 2023

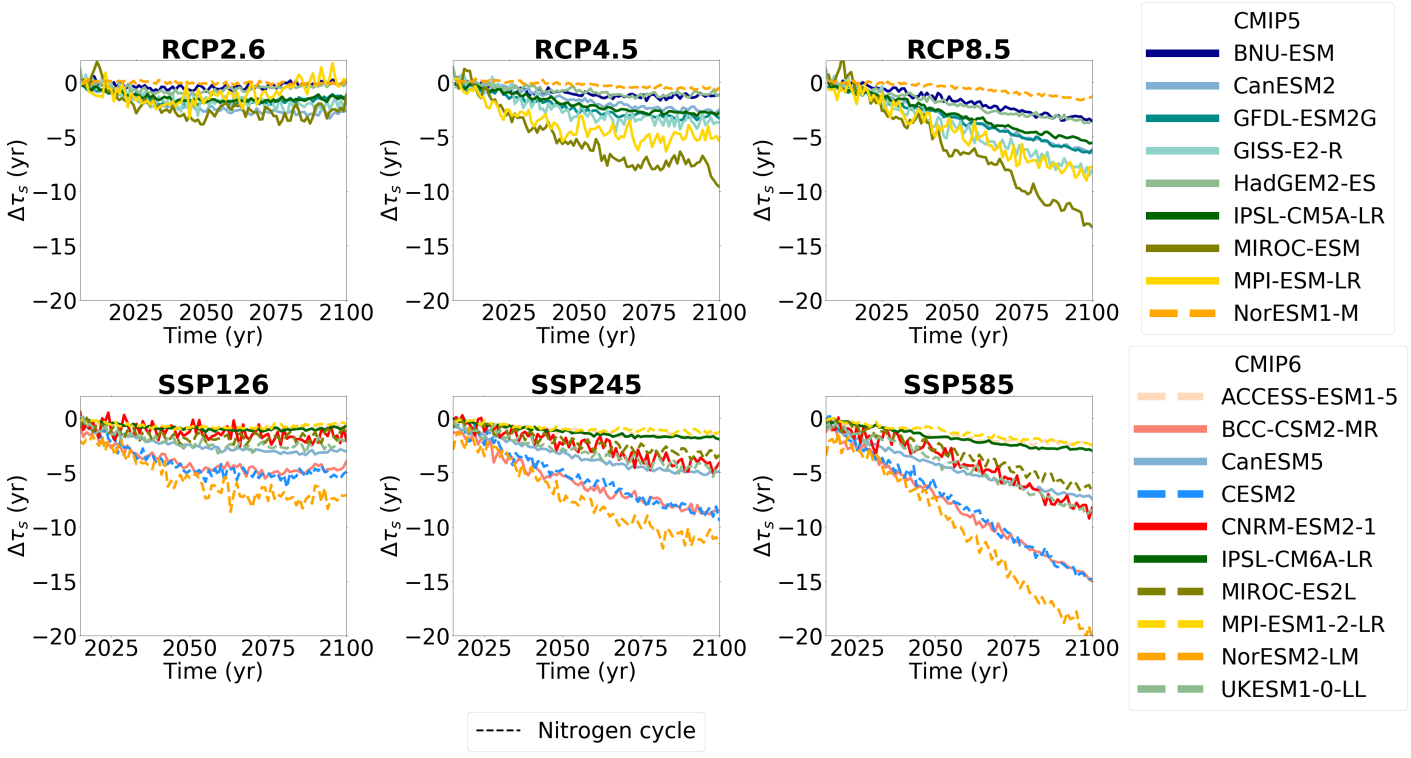

Figure 5. Projected future change in soil carbon turnover time ($\Delta\tau_s$) in CMIP5 (top row) and CMIP6 (bottom row) ESMs, for future climate scenarios *RCP2.6* and *SSP126*, *RCP4.5* and *SSP245*, *RCP8.5* and *SSP585*, respectively. The dashed lines represent ESMs which include the representation of interactive nitrogen in these simulations.

https://doi.org/10.5194/egusphere-2023-383
Preprint. Discussion started: 24 March 2023

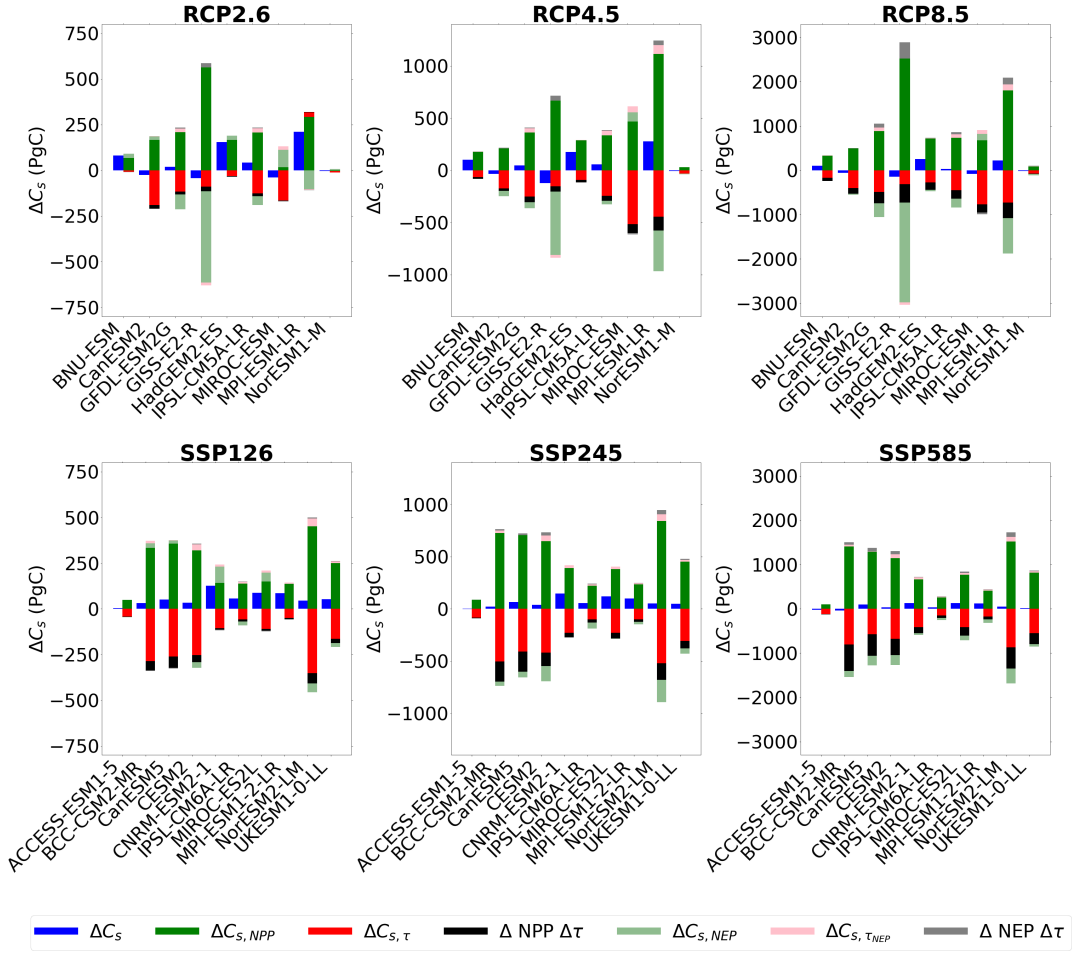

Figure 6. A bar chart showing the contributions of NPP and τ_s to end of 21st century changes in soil carbon (ΔC_s) in CMIP5 (top row) and CMIP6 (bottom row) ESMs, for future scenarios: *RCP2.6* and *SSP126*, *RCP4.5* and *SSP245*, *RCP8.5* and *SSP585*, respectively. The included terms are: the linear term representing changes in soil carbon due to the changes in NPP ($\Delta C_{s,NPP}$), the linear term representing changes in soil carbon due to the changes in τ_s ($\Delta C_{s,\tau}$), the non-linear term ($\Delta\mathrm{NPP}\Delta\tau_\mathrm{s}$), and then additional terms to account for the non-equilibrium climate in 2100 ($\Delta C_{s,NEP}$, $\Delta C_{s,\tau_{NEP}}$, and $\Delta\mathrm{NEP}\Delta\tau_\mathrm{s}$).

https://doi.org/10.5194/egusphere-2023-383
Preprint. Discussion started: 24 March 2023

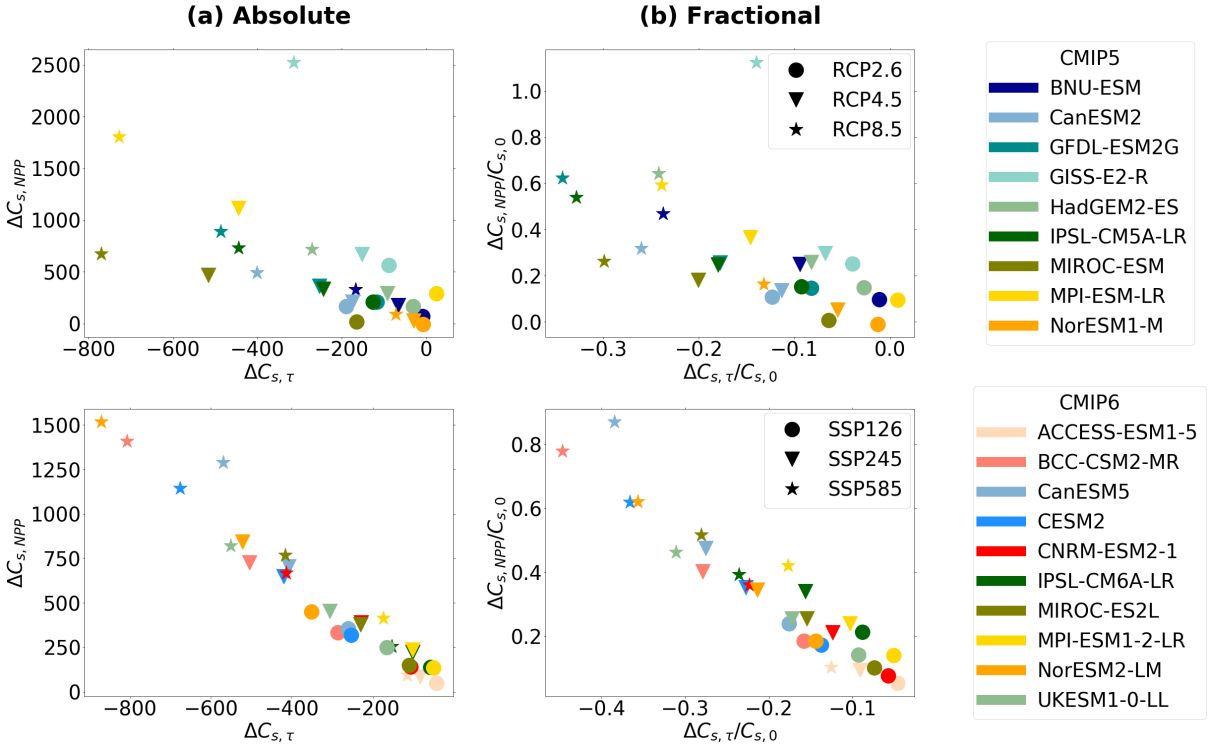

Figure 7. Scatter plot comparing the relationship between $\Delta C_{s,NPP}$ and $\Delta C_{s,\tau}$ for CMIP5 (top row) and CMIP6 (bottom row) ESMs in future scenarios *RCP2.6* and *SSP126*, *RCP4.5* and *SSP245*, *RCP8.5* and *SSP585*, respectively, for (a) absolute changes, and (b) fractional changes.

https://doi.org/10.5194/egusphere-2023-383
Preprint. Discussion started: 24 March 2023

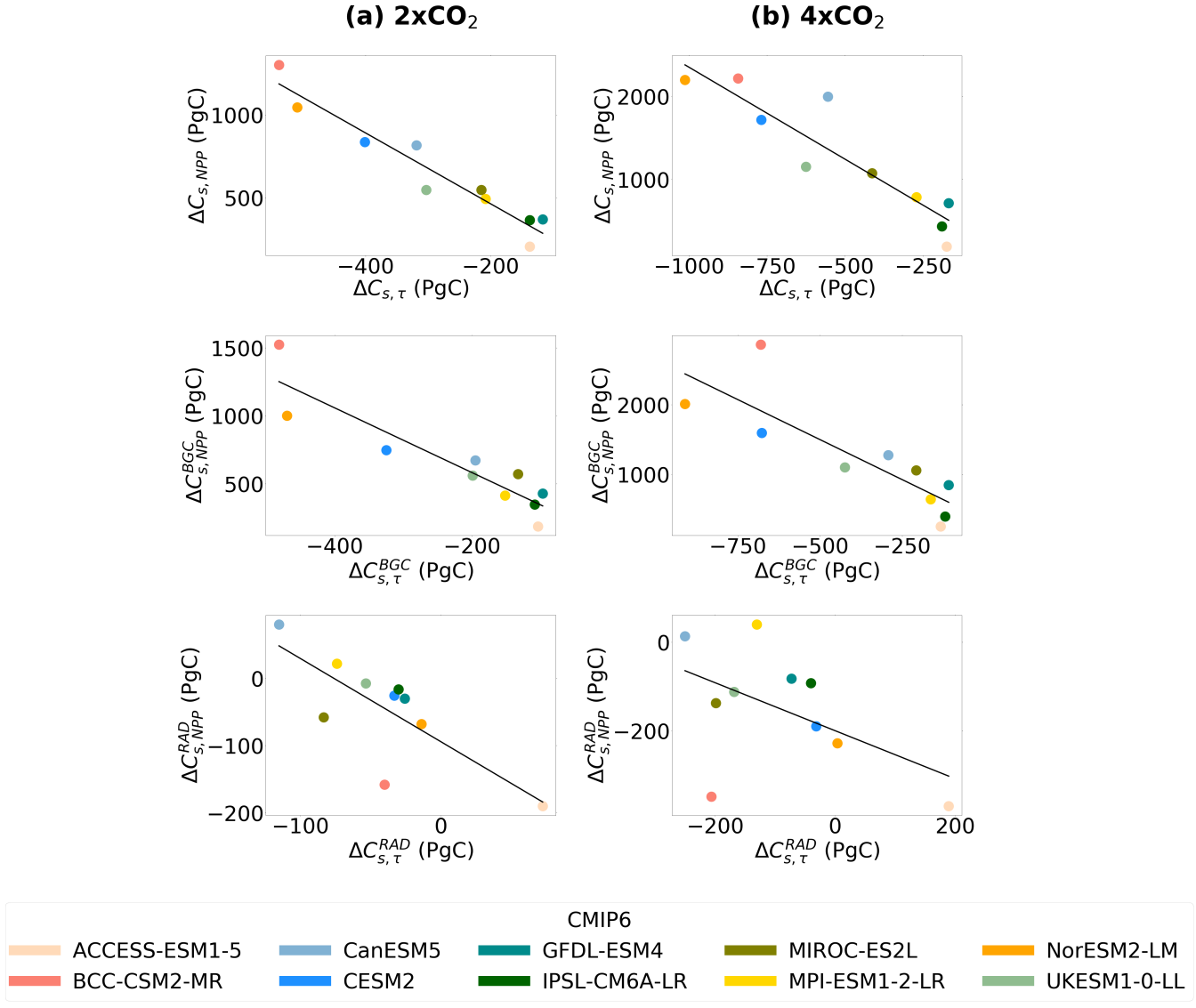

Figure 8. Scatter plots showing the relationship between $\Delta C_{s,NPP}$ and $\Delta C_{s,\tau}$ for each CMIP6 ESM, in the *full* 1% CO_2 simulation (top row), *BGC* simulation (middle row) and *RAD* simulation (bottom row), for (a) 2xCO_2 and (b) 4xCO_2.

https://doi.org/10.5194/egusphere-2023-383
Preprint. Discussion started: 24 March 2023

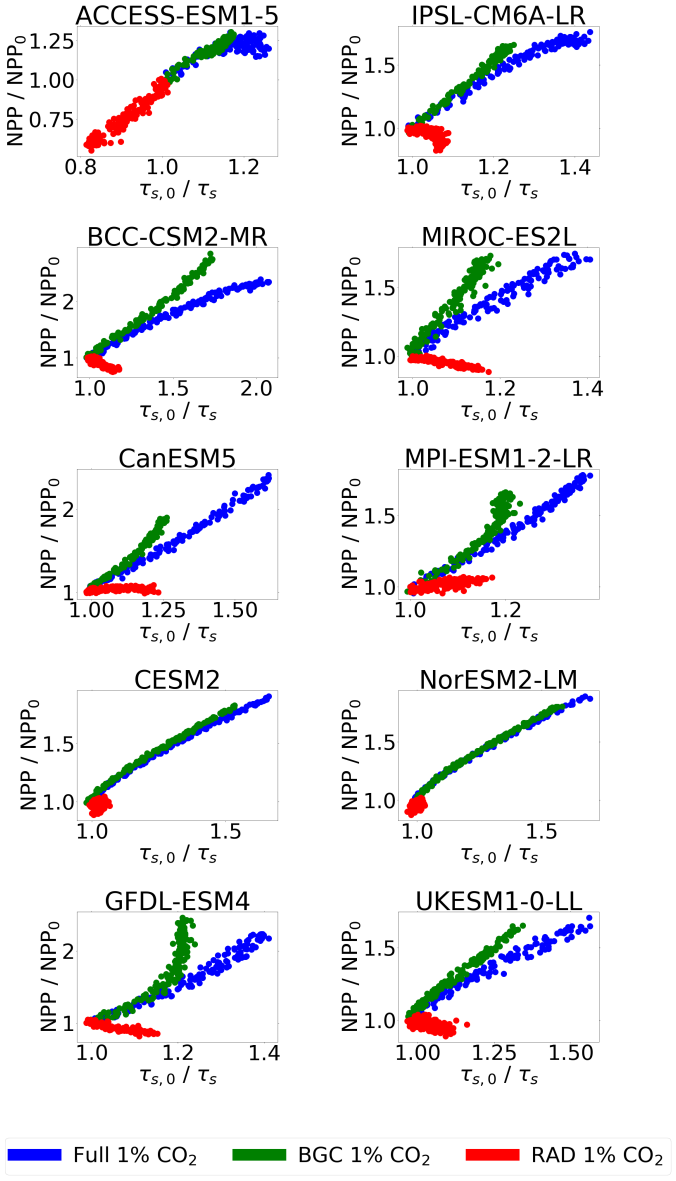

Figure 9. Scatter plots showing the correlation between $\mathrm{NPP}/\mathrm{NPP}_0$ and $\tau_{s,0}/\tau_s$ for each CMIP6 ESM, in the *full* 1% CO_2 simulation (blue) and the *BGC* simulation (green), up to 4xCO_2.

https://doi.org/10.5194/egusphere-2023-383
Preprint. Discussion started: 24 March 2023

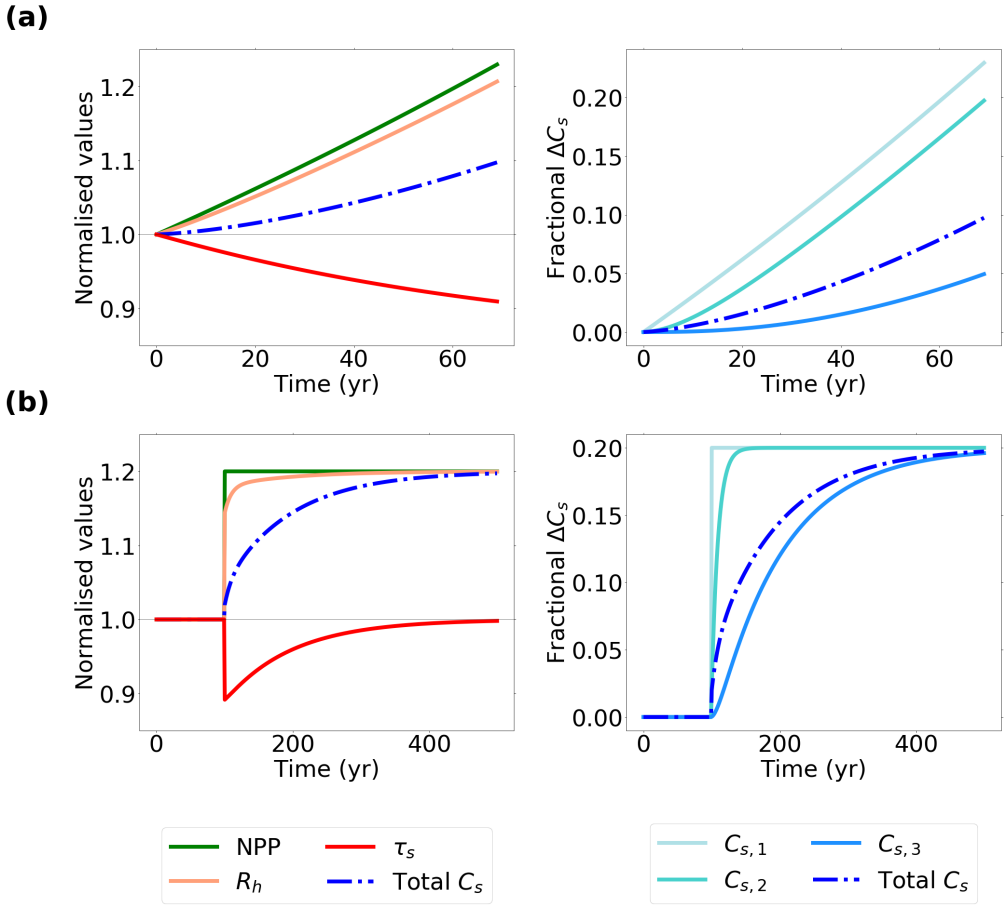

Figure 10. Timeseries plot showing the results from the simple three-box model. (a) For normalised changes in NPP, R_h, τ_s and C_s and fractional change in each of the 3 soil carbon boxes and in the total soil carbon (recreation of Fig. 12 in Koven et al. (2015)). (b) For an abrupt change in global NPP, from 50 PgC yr^{-1} to 70 PgC yr^{-1} at year 100.

https://doi.org/10.5194/egusphere-2023-383
Preprint. Discussion started: 24 March 2023

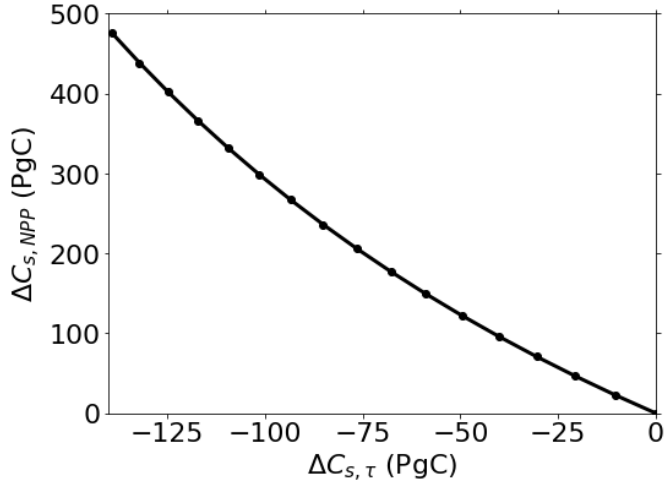

Figure 11. Relationship between $\Delta C_{s,NPP}$ and $\Delta C_{s,\tau}$ derived from the three-box model. Each dot represents the results at the end of a 70 year run with a different assumed rate of increase of NPP ($\sim$ 0.0% to 0.8% per year in increments of 0.05%).

https://doi.org/10.5194/egusphere-2023-383
Preprint. Discussion started: 24 March 2023

Table 1. Table presenting the absolute (PgC) and relative (%) change in 21st century soil carbon (ΔC_s) for each CMIP6 model and the ensemble mean ± standard deviation, for each future SSP scenario.

Earth System Model	Absolute ΔC_s (PgC)			Relative ΔC_s (%)		
	SSP126	SSP245	SSP585	SSP126	SSP245	SSP585
ACCESS-ESM1.5	3.44	-0.98	-23.4	0.38	-0.108	-2.55
BCC-CSM2-MR	31.8	22.3	-35.2	1.76	1.23	-1.95
CanESM5	50.6	66.7	97.7	3.41	4.49	6.59
CESM2	32.7	38.3	32.4	1.77	2.08	1.76
CNRM-ESM2-1	126	145	132	6.79	7.85	7.11
IPSL-CM6A-LR	57.6	55.0	35.5	8.86	8.45	5.46
MIROC-ES2L	87.3	118	126	5.88	7.94	8.5
MPI-ESM1-2-LR	86.2	97.9	123	8.79	9.98	12.5
NorESM2-LM	44.1	52.0	48.7	1.81	2.13	1.99
UKESM1-0-LL	52.3	46.9	17.5	2.96	2.65	0.988
Ensemble mean	55.4	58.3	50.3	4.53	4.24	3.67
± standard deviation	± 31.8	± 44.3	± 57.8	± 2.95	± 3.51	± 4.50

https://doi.org/10.5194/egusphere-2023-383
Preprint. Discussion started: 24 March 2023

Table 2. Table presenting the change in 21st century NPP and τ_s for each CMIP6 model and the ensemble mean $\pm$ standard deviation, for each future SSP scenario.

Earth System Model	ΔNPP (PgC yr^{-1})			$\Delta\tau_s$ (yr)		
	SSP126	SSP245	SSP585	SSP126	SSP245	SSP585
ACCESS-ESM1.5	1.66	3.58	4.07	-0.828	-1.69	-2.35
BCC-CSM2-MR	8.37	19.7	39.4	-4.53	-8.52	-14.0
CanESM5	17.4	35.4	65.8	-3.09	-5.01	-7.10
CESM2	6.46	13.7	24.5	-5.05	-8.63	-14.1
CNRM-ESM2-1	2.28	7.96	14.3	-1.624	-4.19	-8.05
IPSL-CM6A-LR	8.40	13.9	16.2	-0.938	-1.81	-2.83
MIROC-ES2L	4.90	13.9	29.0	-1.52	-3.37	-6.23
MPI-ESM1-2-LR	7.84	14.3	25.9	-0.555	-1.27	-2.30
NorESM2-LM	6.33	12.6	23.3	-7.16	-11.0	-18.9
UKESM1-0-LL	8.08	15.2	28.1	-2.37	-4.52	-8.25
Ensemble mean	7.44	13.6	24.6	-2.30	-4.55	-7.65
$\pm$ standard deviation	$\pm$ 4.01	$\pm$ 8.71	$\pm$ 16.9	$\pm$ 2.047	$\pm$ 3.35	$\pm$ 5.65

https://doi.org/10.5194/egusphere-2023-383
Preprint. Discussion started: 24 March 2023

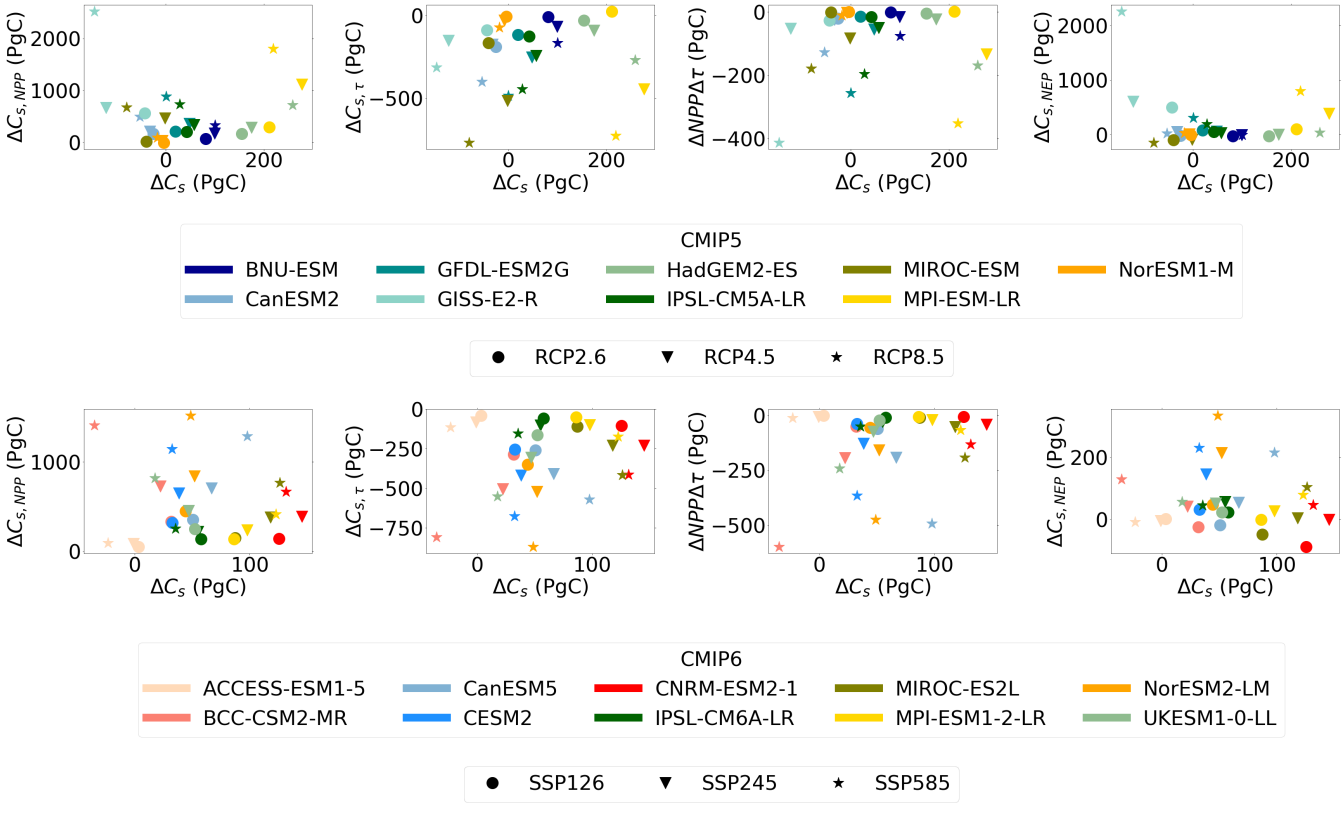

Figure A1. Scatter plot comparing the relationship between $\Delta C_{s,NPP}$, $\Delta C_{s,\tau}$, $\Delta \mathrm{NPP}\Delta\tau_s$, and $\Delta C_{s,\tau_{NEP}}$, each against ΔC_s, for CMIP5 (top row) and CMIP6 (bottom row) ESMs, for future scenarios *SSP126* and *RCP2.6*, *SSP245* and *RCP4.5*, *SSP585* and *RCP8.5*.

https://doi.org/10.5194/egusphere-2023-383
Preprint. Discussion started: 24 March 2023

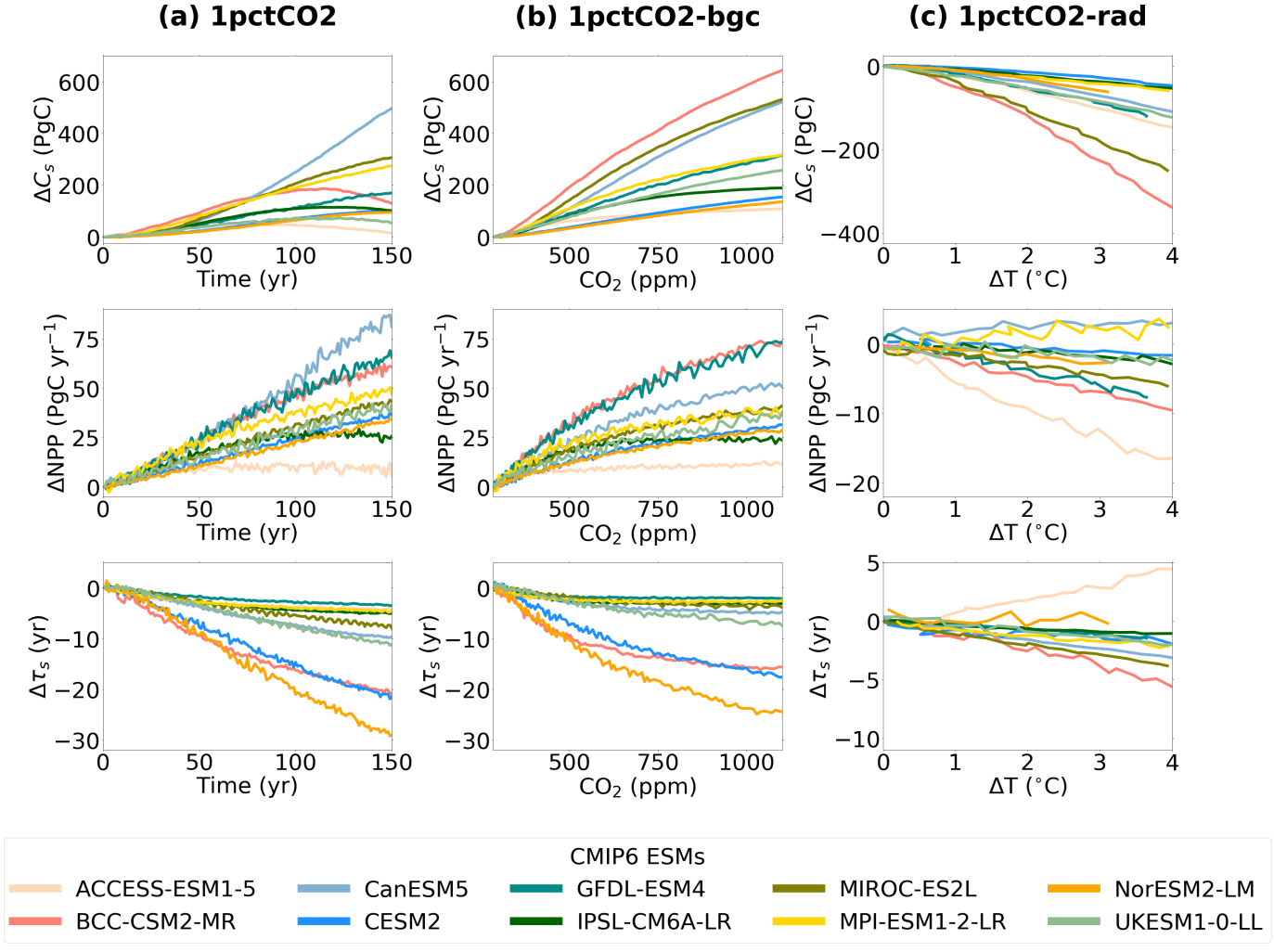

Figure A2. Timeseries of projected changes in Soil carbon (ΔC_s, top row) Net Primary Productivity (ΔNPP, middle row), and soil carbon turnover time ($\Delta\tau_s$, bottom row) in CMIP6 ESMs for the idealised simulations 1% CO_2 (left column), biogeochemically coupled 1% CO_2 (*BGC*, middle column) and radiatively coupled 1% CO_2 (*RAD*, right column).

https://doi.org/10.5194/egusphere-2023-383
Preprint. Discussion started: 24 March 2023

Table A1. Table presenting the absolute (PgC) and relative (%) change in 21st century soil carbon for each CMIP5 model and the ensemble mean ± standard deviation, for each future RCP scenario.

Earth System Model	Absolute ΔC_s (PgC)			Relative ΔC_s (%)		
	RCP2.6	RCP4.5	RCP8.5	RCP2.6	RCP4.5	RCP8.5
BNU-ESM	81.4	99.7	100	11.6	14.2	14.3
CanESM2	-25.4	-32.7	-53.5	-1.65	-2.12	-3.47
GFDL-ESM2G	19.9	47.9	0.278	1.40	3.37	0.020
GISS-E2-R	-43.1	-122	-146	-1.92	-5.43	-6.50
HadGEM2-ES	154	174	258	13.9	15.6	23.2
IPSL-CM5A-LR	42.5	57.1	28.4	3.14	4.22	2.10
MIROC-ESM	-39.9	-1.53	-80.0	-1.55	-0.059	-3.11
MPI-ESM-LR	211	277	219	6.94	9.09	7.19
NorESM1-M	-3.94	-7.60	-17.7	-0.723	-1.40	-3.26
Ensemble mean	44.1	54.7	34.3	3.45	4.17	3.38
± standard deviation	± 84.2	± 111	± 127	± 5.66	± 6.97	± 9.24

https://doi.org/10.5194/egusphere-2023-383
Preprint. Discussion started: 24 March 2023

Table A2. Table presenting the change in 21st century NPP and τ_s for each CMIP5 model and the ensemble mean $\pm$ standard deviation, for each future RCP scenario.

Earth System Model	ΔNPP (PgC)			$\Delta\tau_s$ (yr)		
	RCP2.6	RCP4.5	RCP8.5	RCP2.6	RCP4.5	RCP8.5
BNU-ESM	4.52	11.7	21.9	-0.165	-1.36	-3.42
CanESM2	6.94	8.73	20.4	-2.95	-2.71	-6.23
GFDL-ESM2G	9.47	16.4	40.13	-1.53	-3.31	-6.38
GISS-E2-R	11.5	13.6	51.4	-2.26	-3.88	-8.03
HadGEM2-ES	10.4	18.2	45.5	-0.40	-1.24	-3.66
IPSL-CM5A-LR	10.4	16.9	37.0	-1.50	-2.91	-5.31
MIROC-ESM	0.350	9.98	14.4	-2.66	-8.32	-12.4
MPI-ESM-LR	-	26.6	43.0	-0.280	-5.00	-8.17
NorESM1-M	-0.388	2.25	6.94	-0.151	-0.645	-1.55
Ensemble mean	5.32	12.4	28.1	-1.26	-3.26	-6.13
$\pm$ standard deviation	$\pm$ 4.74	$\pm$ 7.42	$\pm$ 16.8	$\pm$ 1.13	$\pm$ 2.21	$\pm$ 3.03